

1 **An Overview Of The Clinical Applications Of Optical Coherence**  
2 **Tomography Angiography**

3  
4  
5 Authors: Anna C.S Tan<sup>1,2,3</sup>, Gavin S. Tan<sup>1,2,3</sup>, Alastair K. Denniston<sup>4,5,6</sup>,  
6 Pearse A. Keane<sup>6</sup>, Marcus Ang<sup>1,2,3</sup>, Dan Milea<sup>1,2,3</sup>, Usha Chakravarthy<sup>7</sup>,  
7 Chui Ming Gemmy Cheung<sup>1,2,3</sup>

- 8  
9 1. Singapore National Eye Center, Singapore Singapore  
10 2. Singapore Eye Research Institute, Singapore Singapore  
11 3. Duke-NUS Medical School, Singapore, Singapore  
12 4. Department of Ophthalmology, University Hospitals of  
13 Birmingham NHS Foundation Trust, Birmingham, UK  
14 5. Academic Unit of Ophthalmology, Institute of Inflammation &  
15 Ageing, University of Birmingham, Birmingham, UK  
16 6. National Institute for Health Research (NIHR) Biomedical  
17 Research Centre at Moorfields Eye Hospital NHS Foundation  
18 Trust and UCL Institute of Ophthalmology, London, UK.  
19 7. Department of Ophthalmology, Queen's University of Belfast.  
20 Royal Victoria Hospital. Belfast Northern Ireland.

21  
22  
23 **Total word limit: 8080 words**

24 **Figures: 11**

25 **Tables: 3**

26 Correspondence: Gemmy Cheung  
27 Singapore National Eye Center  
28 11 Third Hospital Avenue  
29 Telephone 65 6227 7255  
30 Fax 65 6379 3519  
31 Email: gemmy.cheung.c.m@singhealth.com.sg  
32

34 **Abstract (248 words)**

35 Optical coherence tomography angiography (OCTA) has emerged as a  
36 novel, non-invasive imaging modality that allows the detailed study of  
37 flow within the vascular structures of the eye. Compared to  
38 conventional dye angiography, OCTA can produce more detailed,  
39 higher resolution images of the vasculature without the added risk of  
40 dye injection. In our review, we discuss the advantages and  
41 disadvantages of this new technology in comparison to conventional  
42 dye angiography. We provide an overview of the current OCTA  
43 technology available, compare the various commercial OCTA machines  
44 technical specifications and discuss some future software  
45 improvements. An approach to the interpretation of OCTA images by  
46 correlating images to other multi-modal imaging with attention to  
47 identifying potential artefacts will be outlined and may be useful to  
48 ophthalmologists, particularly those who are currently still unfamiliar  
49 with this new technology.

50

51 This review is based on a search of peer-reviewed published papers  
52 relevant to OCTA according to our current knowledge, up to January  
53 2017, available on the PubMed database. Currently, many of the

54 published studies have focused on OCTA imaging of the retina, in  
55 particular, the use of OCTA in the diagnosis and management of  
56 common retinal diseases such as age related macular degeneration and  
57 retinal vascular diseases. In addition, we describe clinical applications  
58 for OCTA imaging in inflammatory diseases, optic nerve diseases and  
59 anterior segment diseases. This review is based on both the current  
60 literature and the clinical experience of our individual authors, with an  
61 emphasis on the clinical applications of this imaging technology.

62

63

64 **Method**

65 This comprehensive literature review was performed based on a  
66 search of peer-reviewed published papers relevant to optical  
67 coherence tomography angiography (OCTA) according to our current  
68 knowledge, up to January 2017, available on the PubMed database.

69 This review will highlight OCTA technology and software updates  
70 relevant to clinicians and discuss clinical approaches to the  
71 interpretation of OCTA keeping in mind its limitations and artefacts.  
72 We will then examine some current clinical applications of this  
73 technology and implications for future use.

74

75 **Overview of technology**

76

77 OCT angiography (OCTA) is a novel imaging modality that allows the  
78 detailed 3 dimensional study of blood flow within the vascular  
79 structures of the eye without the need to intravenously administer  
80 fluorescent dyes.<sup>1,2</sup> OCTA technology is based on detecting  
81 differences in amplitude, intensity or phase variance between  
82 sequential B-scans taken at the same location of the retina.<sup>1</sup> Briefly, a  
83 series of B-scans are collected at the same transverse location and

84 registered. The degree of decorrelation in signal is then calculated,  
85 which enables visualization of only the moving part, assumed to be due  
86 to movement of cells within the blood stream and thus blood flow. The  
87 above procedure is then repeated for different Y-position in the retina  
88 to achieve the 3D dataset, from which proprietary algorithms such as  
89 split-spectrum amplitude-decorrelation angiography (SSADA), optical  
90 microangiography (OMAG) and OCT angiography ratio analysis  
91 (OCTARA) are used to reconstruct enface angiograms (Figure 1).

92 OCTA offers several advantages compared to conventional  
93 angiography. The non-invasive nature and fast acquisition time allows  
94 this test to be repeated frequently and avoids the potential risks  
95 associated with intravenous dye injection (Table 1). In addition, high-  
96 resolution details of the vasculature and depth-resolved analysis, in  
97 which the flow within a specific axial location of the retinal or choroid  
98 can be analysed (Table 1). The absence of functional information such  
99 as the severity of exudation and filling speed as well as stereoscopic  
100 viewing and wide-field functions (Table 1) are other disadvantages of  
101 OCTA compared to conventional angiography.

102 Automated, objective quantitative measures (angio-analytics) of flow

103 have been incorporated into many OCTA platforms (Table 2.)<sup>3</sup> These  
104 software developments are still in their infancy and need to be tested  
105 for intra- and inter-platform reliability and repeatability, in both  
106 normal and diseased eyes Some instruments offer a function to  
107 ‘register’ two different visits by aligning features on the enface images.  
108 This function is useful for assessing treatment response and disease  
109 progression (Table 2).<sup>4-7</sup>

### 110 **OCTA interpretation and potential artefacts**

111 In our experience, high quality image acquisition for each OCTA  
112 platform has a learning curve; hence good technical support is  
113 essential and poor quality images should be identified. Instrument-  
114 related factors that may affect image quality include differences in  
115 acquisition time. Patient-related factors include age, ability to co-  
116 operate and maintain fixation, and the presence media opacity.

117 Similar to image acquisition, OCTA interpretation by the clinician, also  
118 has a learning curve. The user interfaces of most of the current OCTA  
119 platforms vary, however the basic components are similar. An  
120 approach to OCTA interpretation is outlined below (Figure 2).

121 • *Assess the scan quality*

122 This should include assessment of the scan centration, resolution and  
123 signal strength. Signal strength may be affected by patient co-  
124 operation, fixation or media opacity.

125 • *Identify the layer and the area of interest*

126

127 Through a detailed clinical exam and examination of the structural  
128 OCT, the clinician should be able to determine at which layer (retinal  
129 versus choroidal) the pathology lies and the area of interest to be  
130 scanned by the OCTA, keeping in mind the various scan area options  
131 available on the various OCTA platforms. If the pathology is not around  
132 the macula, an OCTA scan decentred from the fovea may be necessary.

133

134 • *Examine the cross-sectional OCTA for abnormal flow*

135 Most OCTA platforms represent the detected flow signals by  
136 superimposing them onto a structural B-scan OCT images in a coloured  
137 overlay to derive a cross sectional OCTA image (Figure 1). Scrolling  
138 through the cross-sectional OCTA images to look for abnormal flow in  
139 the layer and area of interest will help locate the corresponding area

140 on the enface OCTA to focus on.

- 141 • *Choose the preset segmentation pattern that best captures the area of*  
142 *abnormal flow*

143

144 All the commercially available OCTA instruments are built with  
145 automated segmentation (Table 2). If no particular segmentation  
146 pattern is able to accurately capture the area of abnormal flow, (e.g. for  
147 studying large choroidal vessels or pre-retinal neovascularization),  
148 customized segmentations patterns may be necessary to obtain an  
149 optimized en face OCTA image.

150

- 151 • *Manual manipulation of the segmentation to optimise the en face*  
152 *OCTA image*

153 The exact depth and thickness of the preset segment varies according  
154 to individual instrument. Further manual adjustment of the lower and  
155 the upper boundaries of various segmentation patterns will allow the  
156 enface OCTA image to be easily tailored towards the clinical question.

157 In some pathological cases, where the anatomy is severely disrupted,  
158 automated segmentation may not be accurate and the adjustment of

159 the contour on each of the individual B scan segmentation lines may be  
160 required to optimize the en face OCTA image (Figure 3D). This manual  
161 adjustment of the contour is both time and labour intensive. However  
162 upgrades in the software, such as auto-propagation of manual changes  
163 have shortened the time to perform such adjustments may improve  
164 this function.

165 *Correlate to other imaging modalities*

166 OCTA is a new technology, which has yet to be validated; hence  
167 interpretation should be done with caution and in equivocal cases  
168 correlation with more conventional modalities such as fundus  
169 fluorescein angiography (FA) or indocyanine green angiography  
170 (ICGA).

171 • *Be mindful of artefacts*

172 Understanding the types and sources of artefacts is important during  
173 the interpretation of OCTA (Figure 3).<sup>8,9</sup> Motion artefacts caused by  
174 blinking results in dark lines, while motion artefacts due to saccadic  
175 eye movements or bulk movements usually appear as horizontal white  
176 lines and can be minimized with a few strategies such as orthogonal

177 image registration (Figure 3A),<sup>9,10</sup> the incorporation of an eye-tracker  
178 or a combination of tracking assisted scanning integrated with motion  
179 correction technology (Table 2).<sup>11</sup> In theory, less motion artefact  
180 should occur with a more sensitive the eye-tracker; however a highly  
181 sensitive eye tracker may increase the acquisition time and make  
182 imaging challenging.

183 As previously stated, segmentation errors are common in pathology, in  
184 which the retinal architecture is altered. Inaccurate segmentation may  
185 result in dark areas on the enface OCTA image (Figure 3D). Scrolling  
186 through the structural OCT volume scan will allow identification of  
187 areas with inaccurate segmentation. Manual adjustment should be  
188 performed before interpretation of the final en face OCTA.

189 Projection artefacts occur in highly reflective layers of the retina such  
190 as the retinal pigment epithelium (RPE) (Figure 3B).<sup>8,9,12,13</sup> When  
191 superficial retinal flow signals (Figure 3B-green box) are reflected off  
192 the deeper layers, they will be detected as decorrelation signals that  
193 possess the same character as overlying blood vessels. (Figure 3B-  
194 yellow box).<sup>12</sup> As a result, flow may be inaccurately interpreted to be  
195 present within a deeper structure, when the flow signals actually

196 originated from the more superficial layers. Most OCTA platforms  
197 possess in-built software to mask the projection artefacts in the outer  
198 retinal layers.<sup>14</sup> However, this software has limitations, as projection  
199 artefacts may occur in various other layers, especially in  
200 hyperreflective pathological structures such as hard exudates and  
201 subretinal fibrosis.<sup>14,15</sup> A useful way to ascertain whether the flow  
202 signal seen is due to projection artefact is by examining the cross  
203 sectional OCTA (or Angio B scan), in which the linear signals can be  
204 traced to flow within a more superficial layer (Figure 4).

205 Masking artefacts in the choroidal layers may be caused by blocked  
206 flow signals from overlying hyper-reflective structures, slow flow,  
207 which is below the detectable threshold or a possible segmentation  
208 error.<sup>13,15</sup> On the other hand, unmasking artefacts are seen when areas  
209 of RPE atrophy allow the back-scatter, decorrelation signal of the  
210 underlying choroidal vessels to be seen as areas of increased flow  
211 within the choroid (Figure 3C).<sup>13</sup> On cross sectional OCTA, the high  
212 flow signal is seen directly under the areas where the hyperreflective  
213 RPE band is disrupted (Figure 3C). On en face OCTA, the boundaries of  
214 the high flow area sharply correspond to the areas of RPE loss and this  
215 a further confirmed on comparison to fundus autofluorescence (FAF),

216 where the high flow area corresponds to the area of  
217 hypoautofluorescence due to RPE atrophy (Figure 3C). Other artefacts  
218 described such as the fringe washout effect and the stromal  
219 decorrelation signal, may help explain the differences in the vascular  
220 appearance in normal eyes of the choroidal vessels, which appear dark  
221 compared to the surrounding stroma versus retinal vessels that appear  
222 bright.<sup>13</sup>

223

## 224 **OCTA in age related macular degeneration and other choroidal** 225 **diseases**

226 Many studies have evaluated OCTA in the diagnosis and monitoring of  
227 treatment response in neovascular AMD.

228

## 229 **OCTA findings in choroidal neovascularization (NV)**

230

### 231 ***Type 1 NV***

232 OCTA may allow better visualization of the vascular structure of the  
233 type 1 NV compared to FA, as there is less masking from the overlying

234 RPE and the vasculature is not obscured by dye leakage.<sup>16</sup> The OCT

235 appearance of a type 1 NV is characterised by a vascularised pigment  
236 epithelial detachment (PED) with an irregular surface and  
237 hyperreflective contents. On cross sectional OCTA, intrinsic flow is  
238 seen within the contents of the PED in the sub-RPE space (Figure 4A).<sup>17</sup>  
239 In the corresponding enface OCTA, typically, type 1 NV appears as a  
240 well-defined tangle of vessels (Figure 4A).<sup>17-19</sup> Compared to FA,  
241 previous retrospective case series have reported that OCTA can detect  
242 Type 1 NV in 67-100% of cases.<sup>18-20</sup> Compared to mid- or late phase  
243 ICGA, the appearance of Type 1 NV on OCTA has been noted to occupy  
244 significantly smaller areas.<sup>21</sup>

245

#### 246 ***Type 2 NV***

247 An active type 2 NV appears as subretinal hyper-reflective material  
248 (SHRM) above the RPE with intrinsic flow signals on cross sectional  
249 OCTA (Figure 4B)<sup>15,22</sup>. The hyper-flow patterns detected, that were  
250 described as either a glomerulus or a medusa shape, were associated  
251 with a thicker main vessel branch connected to the deeper choroid.<sup>22</sup> A  
252 dark halo surrounding the lesion was thought to correspond to  
253 masking from surrounding, blood, exudation or subretinal fibrosis.<sup>22</sup> Of  
254 note, the high flow signal was also shown in some cases to cause a

255 projection artefact onto the deeper choriocapillaris layer.<sup>22</sup>

256

257 Mixed type 1 and type 2 lesion can be observed as abnormal flow seen  
258 both above and below the RPE on cross sectional OCTA (Figure 6B).<sup>23</sup>

259 By varying the depth of segmentation, both the more superficial  
260 subretinal type 2 component and the deeper sub-RPE type 1

261 component can be seen on en face OCTA as a vascular network. A

262 previous paper described a larger decrease in the area of the type 2

263 component compared to the type 1 component in response to anti-

264 VEGF therapy.<sup>23</sup>

265

### 266 ***Retinal Angiomatous proliferation (Type 3 NV)***

267

268 Typical OCT findings of type 3 NV show a linear hyper-reflective

269 structure extending from the outer retina to the inner retinal layers,

270 with or without PED. Cross-sectional OCTA of type 3 NV showed

271 intrinsic flow within this structure and 2 patterns of flow were

272 observed; either a discrete intra-retinal flow signal or a linear flow

273 signal that extended from the intra-retinal areas deep through to the

274 RPE band (Figure 4C).<sup>24</sup> En face OCTA of the type 3 NV, showed a

275 bright high flow tuft of microvessels originating from the deep  
276 capillary plexus in the outer retina.<sup>24,25</sup> Distinct neovascular complexes  
277 could only be imaged in 34% of eyes, all of which showed signs of  
278 activity on OCT.<sup>25,26</sup>

279

### 280 ***Progression of neovascularization in response to treatment***

281 Various terminologies have been proposed to describe features that  
282 reflect different stages or level of activity within a neovascular  
283 network. However, there is lack of standardization and validation, so  
284 these terms are likely to undergo further refinement. While OCTA  
285 cannot evaluate the presence of leakage or exudation, changes in  
286 pattern of vasculature on OCTA have been reported as the NV evolves  
287 from active to inactive stages. Characteristic features suggestive of an  
288 active NV include presence of a tangle of vessels in a well-defined  
289 shape (lacy-wheel or sea fan), branching, numerous tiny capillaries, the  
290 presence of anastomoses or loops, the presence of a peripheral arcade  
291 and the presence of a hypointense halo (Figure 5B).<sup>27</sup> In contrast,  
292 inactive chronic NVs have larger more mature vessels, a “dead tree”  
293 appearance with the absence of the anastomoses, loops and peripheral  
294 arcades.<sup>27</sup> After intravitreal anti-VEGF therapy NV showed a decrease in

295 vessel density, vessel fragmentation and the loss of peripheral  
296 capillaries after 1 week with recurrence of the peripheral anastomosis  
297 and increased capillary density at 4 weeks.<sup>28 29</sup> Finally, chronic NV may  
298 show little anatomical response to anti-VEGF (Figure 5B)<sup>18</sup>. On OCTA,  
299 the lesion area and vessel density have been observed to remain  
300 unchanged and the vascular tangle may develop a pruned tree  
301 appearance.<sup>18,25</sup> These fibrovascular PEDs that had undergone multiple  
302 previous treatments, demonstrated prominent vascular loops and  
303 anastomotic connections and showed trunk feeder vessels of a large  
304 diameter with limited branching patterns.<sup>30</sup>

305

306 In response to anti-VEGF therapy, type 3 NVs on OCTA showed a  
307 significant regression in the small calibre tufts in all eyes, with a  
308 reduction in median lesion area and exudation.<sup>6,26</sup> In 29% of eyes, the  
309 high flow lesion became undetectable after a single intravitreal anti-  
310 VEGF injection, however in 65% of eyes there was persistence of the  
311 large feeder vessels.<sup>6</sup> Longitudinal imaging of type 3 NV also showed  
312 that OCTA could detect changes in the vascular complex even before  
313 the presence of exudation seen on OCT, and this may represent early  
314 recurrence. It was also noted that OCTA enabled the distinction

315 between hyper-reflective vascular structures of the type 3 NV from  
316 other surrounding hyper-reflective foci devoid of flow, which may  
317 correlate to pigment migration.<sup>5</sup>

318

319 **OCTA findings in polypoidal choroidal vasculopathy (PCV) and**  
320 **other pachychoroid conditions**

321

322 ICGA is a useful modality for diagnosing PCV. Previous studies show  
323 that OCTA is comparable to ICGA for the detection of BVN.<sup>31-36</sup> In  
324 contrast, the rate of polyp detection by OCTA was much more variable  
325 ranging from 17-85%.<sup>33,34,36,37</sup> Using cross-sectional OCTA, most  
326 studies report the BVN to be in the sub RPE space between the RPE  
327 and Bruch's membrane,<sup>31-33,35</sup> however in one study, some BVNs  
328 associated with PCVs were located deeper within the choroid (Figure  
329 6A)<sup>33</sup>. En face OCTA of the BVN often show networks of vessels in much  
330 more detail than ICGA (Figure 6A).<sup>31-36</sup> Cross sectional OCTA of the  
331 polyp, showed patchy flow signals within the polyp with the lumen  
332 being largely devoid of flow signals. <sup>31,33,35</sup> Enface OCTA imaging of the  
333 polyps was reported to show a more common hypoflow round  
334 structure (75%) or less common (25%) hyperflow round structure

335 surrounded by a hypointense halo.<sup>36</sup> Polyp area measured on OCTA  
336 was also noted to be consistently smaller when compared to ICGA.<sup>37</sup>  
337 Some authors hypothesize that the slow or turbulent flow within the  
338 polyp may explain the hypoflow appearance.

339

340 One study using ss-OCTA imaging showed that in response to anti-  
341 VEGF therapy and in some cases combined photodynamic therapy,  
342 there was a reduction in flow within the PCV complex in most eyes.<sup>34</sup> In  
343 several eyes, despite the improvement in exudation, the ss-OCTA  
344 appearance of the vascular network was unchanged.<sup>34</sup> Changes in the  
345 appearance of the vascular network, which may represent early  
346 recurrence on OCTA may occur even without significant changes on  
347 OCT.<sup>34</sup> Despite quiescence of lesions, as determined on OCT by the  
348 absence of exudation, 88% showed the persistence of flow signals  
349 within the vascular network and this may be a risk factor for  
350 recurrence.<sup>34</sup>

351

352 For all NVs and PCV, longitudinal changes in the flow detected on OCTA  
353 appeared to highly correlate with level of exudation assessed by  
354 structural OCT. In addition, many studies have now demonstrated that

355 the flow signal often persists even though there is absence of fluid, or  
356 within a fibrosed scar.<sup>38</sup>

357

### 358 **Additional OCTA findings in AMD**

359

360 Studies based on OCTA have reported that 6-15% of eyes with chronic  
361 CSC have an associated type 1 NV often seen as a shallow irregular  
362 PED.<sup>20,39</sup> One study reported that OCTA was more sensitive at detecting  
363 vascularised PEDs associated with chronic CSC when compared to dye  
364 angiography.<sup>40</sup>

365

366 Quiescent NV refers to NV detected on conventional angiography such  
367 as FA or ICGA, which shows the absence of exudation.<sup>41</sup> FA shows an  
368 ill-defined hyperfluorescent lesion with no leakage, while ICGA shows  
369 the presence of a hypercyanescent “plaque”.<sup>41</sup> OCTA was reported to  
370 have a sensitivity of 81.8% in quiescent NV detection.<sup>41</sup> Another study  
371 examining eyes with intermediate AMD with the fellow eye having  
372 neovascular AMD, showed 27% of eyes with intermediate AMD had the  
373 presence of a “plaque” on ICGA and a corresponding network of vessels  
374 on ss-OCTA.<sup>42</sup> Another similar study, showed 6% of eyes were found to

375 have the presence of type 1 NV on OCTA, despite no leakage on FA and  
376 exudation on OCT.<sup>43</sup> The clinical significance of these non-exudative,  
377 vascular networks remains to be determined and it has been suggested  
378 that they develop in response to retinal ischemia. It has also been  
379 noted that some of these non-exudative networks will develop frank  
380 exudation during follow-up and thus represent the first signs of early  
381 CNV development. OCTA now provides a method to repeatedly image  
382 non-invasively these networks of dormant vessels and thus provide  
383 insights into the natural history of such lesions.

384

385 In eyes with the presence of subretinal fibrosis secondary to  
386 neovascular AMD, 94% of eyes showed the presence of abnormal flow  
387 signals within the area of fibrosis.<sup>38</sup> Further longitudinal studies are  
388 required to determine the significance of these findings.

389

390 In early AMD, previous studies suggest there maybe a generalised  
391 reduction in choriocapillaris density compared to normal age matched  
392 controls.<sup>44</sup> Due to the shadowing effect of drusen and PEDs, ss-OCTA  
393 has been suggested as the modality of choice due to better penetration  
394 and less shadowing.<sup>42-44</sup> In advanced AMD with geographic atrophy

395 (GA), due to a loss in the RPE and choriocapillaris, the changes in the  
396 underlying choroid are well seen on OCTA.<sup>44</sup> Another study using ss-  
397 OCTA, reported that both focal and diffuse choriocapillaris flow  
398 impairment occurred in eyes with both nascent GA and drusen  
399 associated GA.<sup>45</sup> In addition to the choroidal circulation, AMD can also  
400 cause vascular density reductions in the superficial and deep retinal  
401 plexuses when compared to controls.<sup>46</sup>

402

#### 403 **OCTA in eyes with high myopia**

404 OCTA imaging in eyes with pathologic myopia may help differentiate  
405 between complications such secondary choroidal neovascularisation  
406 where an abnormal flow is seen within the SHRM on cross-sectional  
407 OCTA corresponding to a hyper-flow vascular network seen on en face  
408 OCTA from a simple haemorrhage where no flow or vascular network  
409 is observed.<sup>47</sup> Previous studies have also indicated that in highly  
410 myopic eyes where general thinning of the retinal and choroidal layers  
411 are common, OCTA shows an overall reduced retinal capillary and  
412 choriocapillary density.<sup>48,49</sup> However, OCTA imaging in eyes with high  
413 myopia is challenging due to the steep curvature of the staphyloma  
414 causing poor focus or segmentation errors, areas of myopic

415 degeneration can also lead to unmasking artefacts and difficulty  
416 imaging choroidal flow.<sup>50</sup>

417

### 418 **OCTA in retinal vascular diseases**

419 OCTA in the imaging of vascular diseases has a few important  
420 applications. In the macular region, OCTA allows good delineation of  
421 the foveal avascular zone (FAZ) <sup>51-54</sup> and allows the detection of  
422 macular ischaemia and microaneurysms (Figure 7). In the peripheral  
423 retina, areas of capillary drop out and the detection of  
424 neovascularisation at the disc and elsewhere can also be imaged well  
425 on OCTA (Figure 8).

426

### 427 ***Diabetic eye disease***

428

429 Microaneurysms can be identified in the superficial and deep retinal  
430 capillary plexi and appear as focally dilated saccular or fusiform  
431 capillaries (Figure 7A). Studies to-date suggest that there is often  
432 disagreement between identification of microaneurysm on OCTA and  
433 FA and even between different OCTA platforms.<sup>52</sup> Not all  
434 microaneurysms seen on FA can be found on OCTA, and vice versa

435 some of the dilated capillary changes on OCTA that resembled  
436 microaneurysms are not found FA.<sup>55</sup> Most studies noted more  
437 microaneurysms on FA than OCTA<sup>52,56</sup>, however, Peres et al noted that  
438 OCTA of the DCP had more microaneurysms than either FA or the SCP  
439 on OCTA.

440

441 Comparison of FA and OCTA has demonstrated that OCTA allows  
442 better discrimination of the FAZ and parafoveal microvasculature than  
443 FA, in particular for FAZ disruption, enlargement and capillary dropout  
444 <sup>52</sup>(Figure 7B). In diabetic retinopathy, the outline of the FAZ may  
445 become irregular, with enlarged perivascular spaces and disruption of  
446 the capillary ring. The increase in FAZ area, present in both the  
447 superficial and deep retinal plexi, can precede the development of  
448 clinical diabetic retinopathy, suggesting that diabetic eyes show  
449 impairment of the retinal microcirculation before retinopathy  
450 develops.<sup>57,58</sup> The FAZ area was also found to increase with the  
451 presence of clinically significant macular oedema (Figure 7B), however  
452 there was no statistically significant difference in FAZ area between  
453 eyes with non-proliferative and proliferative diabetic retinopathy. It is  
454 important to note that variations in axial length can affect the retinal

455 vessel magnification on OCTA. Adjustment can be made if axial length  
456 measures are available. Some strategies to quantify the irregularity of  
457 the FAZ independent of axial length include an acircularity index,  
458 defined as the ratio of the perimeter of the FAZ to the perimeter of a  
459 circle with an equal area and an axis ratio, defined as the ratio between  
460 the major and minor axis of an ellipse defined by custom software.<sup>53</sup>  
461 Krawitz et al demonstrated that both the acircularity index and axis  
462 ratio increase with diabetic retinopathy severity and may have  
463 potential to characterize disease severity.<sup>53</sup> These structural changes  
464 on OCTA in diabetic eyes have also been correlated with function.  
465 Balaratnasingam et al described the correlation between larger FAZ  
466 area and worse visual acuity in eyes with diabetic retinopathy. Samara  
467 et al found that visual acuity also correlated with FAZ area, vessel area  
468 density and vessel length density on OCTA.<sup>59</sup>

469

470 OCTA can also identify neovascularization associated with diabetic  
471 retinopathy or retinal vein occlusions (Figure 8). Serial OCTAs can  
472 been used to monitor the change in area of disc neovascularization in  
473 response to treatment with anti-VEGF injections<sup>60</sup>. When  
474 appropriately used, OCTA can also identify the presence of ischemia

475 and neovascularization in the retina mid periphery; and differentiate  
476 new vessels which tend to be anterior to the internal limiting  
477 membrane, from collaterals and intra retinal microvascular  
478 abnormalities.<sup>61</sup>

479

480 Quantitative tools have been developed to quantify areas of retinal  
481 perfusion on OCTA. Capillary fall out in the area surrounding the FAZ  
482 can be readily identified, and may exceed that identified on FA, as these  
483 areas can be masked by diffuse fluorescein leakage.<sup>62</sup> Retinal  
484 vasculature on OCTA can be skeletonized or binarised to define the  
485 total capillary length or luminal area. Various measures of capillary  
486 density based on ratio of luminal area to total area have also been  
487 described.<sup>63-66</sup> Good repeatability and reproducibility of FAZ area and  
488 capillary density on OCTA have been demonstrated in normal eyes.<sup>67</sup> In  
489 normal eyes, with increasing age, capillary density was found to  
490 decrease while the FAZ area increases.<sup>67</sup> Studies have consistently  
491 described lower capillary density in diabetic eyes compared with  
492 controls in both the deep and superficial layers. There was also a  
493 consistent trend of decreasing capillary density with retinopathy  
494 severity.<sup>63,64,66</sup> Automated algorithms to detect the avascular area on

495 OCTA was not only shown to be highly repeatable and reproducible  
496 with the coefficient of variation reported to be less than 7.0%<sup>63</sup> but  
497 could also be used to distinguish mild NPDR from normal eyes.<sup>65</sup> Other  
498 authors who have examined capillary density and vascular measures  
499 such as fractal dimension have also demonstrated a similar trend with  
500 severity of DR<sup>64,66</sup>. Ting et al also demonstrated that hyperlipidemia,  
501 smoking and renal impairment were associated with capillary density  
502 decrease while increased HbA1c and renal impairment were  
503 associated with a increased fractal dimension in diabetic eyes,  
504 suggesting the link between vascular risk factors and preclinical retinal  
505 microvascular changes seen on OCTA.<sup>66</sup>

506

507 In diabetic macular oedema (DMO), OCTA has been used to assess the  
508 baseline characteristics as well as response to anti-VEGF injections  
509 (Figure 7B). Lee et al found that DMO eyes had more microaneurysms  
510 in the capillary plexus, a lower vascular flow density and a larger FAZ  
511 area in the DCP than eyes without DMO. DMO eyes, which were poor  
512 responders to anti-VEGF treatment had a significantly larger FAZ area  
513 and more microaneurysms in the deep capillary plexus on OCTA  
514 compared to eyes that responded well to anti-VEGF treatment. This

515 suggests that the deep capillary plexus is important in DMO occurrence  
516 and may be a useful prognostic tool for predicting anti-VEGF treatment  
517 response in DMO. Another study examining OCTA in DMO did not  
518 demonstrate any change in FAZ area after the treatment of macular  
519 oedema with a single injection of anti-VEGF. <sup>54</sup>

520

### 521 ***Retinal vascular occlusions***

522

523 OCTA can be used to confirm the clinical diagnosis of both retinal vein  
524 and artery occlusions.<sup>68,69</sup> Similar to its utility in DR, OCTA is able to  
525 identify capillary non-perfusion, retinal ischemia, collateral vessels,  
526 capillary telangiectasia and microaneurysms, in addition to delineating  
527 the FAZ in macular ischemia secondary to retinal vein occlusion (RVO)  
528 (Figure 8A&B).<sup>61,70 69,71-74</sup> It has been noted that in RVO, the  
529 microvascular changes on OCTA are more prominent in the deep  
530 retinal plexus than in the superficial plexus.<sup>72</sup> The FAZ area and vessel  
531 density on OCTA have been found to correlate with strongly with  
532 visual acuity in RVO both before and after treatment with anti-VEGF  
533 injections.<sup>75,76 70</sup> OCTA has also been used to follow-up RVO after  
534 treatment, and demonstrated reduction of areas of non-perfusion and

535 capillary disruption after treatment with anti-VEGF injections.<sup>77</sup> In  
536 retinal artery occlusion (RAO), OCTA is able to delineate the extent of  
537 macular non-perfusion and follow-up changes in the vascular flow over  
538 time, and it also revealed perfusion defects in the superficial capillary  
539 plexus, which were not seen on FA.<sup>68</sup> The development of  
540 neovascularisation in an ischaemic RVO can also be detected on OCTA  
541 (Figure 8C)

542

543 Retinal vascular disease affects both the macular and the peripheral  
544 retinal vasculature, and therefore the constraints in imaging of the  
545 peripheral retina with OCTA will limit its utility. OCTA is also unable to  
546 identify areas of focal leakage unlike FA and is dependent on a  
547 cooperative patient with reasonable fixation to produce high quality  
548 images. Segmentation in eyes with macular oedema can also be  
549 challenging and can affect the interpretation of the retinal capillary  
550 plexus, with as many as 22% of images being unreadable.<sup>54,59</sup>

551

### 552 ***Macular telangiectasia***

553 In macula telangiectasia type 1 (MacTel1), a predominantly unilateral  
554 disease, previous studies have reported focal microvascular dilatation

555 and both global and focal capillary depletion when compared to the  
556 fellow eye and normal controls.<sup>78</sup> Volume rendered OCTA images of  
557 eyes with macula telangiectasia type 2 (MacTel2) suggested that the  
558 microvascular changes maybe due to vascular invasion and retinal  
559 thinning and secondary subretinal neovascularisation originate in the  
560 retinal circulation but could infiltrate both the subretinal space and the  
561 overlying thinned retina.<sup>79</sup> The contraction of the tissue surrounding  
562 the temporal macula in the presence of stellate arranged vessels may  
563 explain the origin of the right-angle veins.<sup>80</sup> OCTA was also able to  
564 study the progression of MacTel2 and showed that an increase in the  
565 inter-vascular spaces, capillary rarefaction and increasing abnormal  
566 areas of anastomosis was associated with a reduced capillary density  
567 in the superficial and deep layers when compared to controls.<sup>81,82</sup>

568

### 569 **OCTA in inflammatory diseases**

570

571 Imaging in inflammatory eye diseases has a number of key roles: (1)  
572 detection – i.e. to identify the presence of an inflammatory process; (2)  
573 diagnosis – i.e. to identify the type of inflammation; (3) monitoring –  
574 i.e. to evaluate disease activity and damage.<sup>83</sup> Although OCTA has a role

575 to play in all three domains, it is emerging as a particularly valuable  
576 tool in the area of monitoring. In particular, it is proving valuable in  
577 two key areas where other imaging techniques sometimes fall short:  
578 (1) the need to differentiate between active inflammatory lesions,  
579 active vascular lesions and inactive fibrotic lesions – highlighted by  
580 difficult treatment decisions in conditions such as Punctate Inner  
581 Choroidopathy (PIC); and (2) the need to quantify inflammatory  
582 activity, both to stratify treatment and to monitor response to  
583 treatment.

584

585 Review of the literature in this field identifies short case series and  
586 individual case reports, many of which highlight the additional value of  
587 OCTA as part of a multimodal approach. Although no formal  
588 prospective trials to assess its diagnostic utility in uveitis are yet  
589 available, the studies discussed below show how particular clinical  
590 indications or disease groups may benefit from the additional  
591 information provided by OCTA.

592

593 **Clinical scenarios**

594

595 ***Uveitic Macular Oedema***

596 As one of the leading causes of sight loss in uveitis, uveitic macular  
597 oedema (UMO) is of particular interest, although some caution is  
598 required in OCTA interpretation as extensive oedema may hamper  
599 visualisation and induce artefact. Few studies are available thus far,  
600 but it is interesting to note that in an analysis of 25 eyes with UMO,  
601 Kim et al report significantly lower vessel density in the deep retinal  
602 plexus in eyes with UMO (vs non-UMO uveitic eyes).<sup>84</sup> This preliminary  
603 evidence would support the hypothesis that the leakage in UMO is not  
604 entirely due to increased permeability from inflammatory mediators,  
605 but does include an ischaemic element.

606

607 ***Retinal vasculitis***

608 Assessing disease activity in retinal vasculitis is challenging. It is  
609 usually based on FA with a particular regard to leakage, but also other  
610 vascular abnormalities such as progression of ischaemia. Specific  
611 limitations of FA in this context are (1) leakage of dye in FA may limit  
612 assessment of capillary 'drop-out' due to ischaemia, and (2) damaged  
613 retinal vasculature frequently remains leaky limiting reliable  
614 assessment of disease activity. OCTA has the advantages of being able

615 to assess both structure and perfusion of the microvasculature without  
616 being obscured by leakage. It does have the disadvantage of not  
617 directly assessing leakage, which subject to the limitations above, may  
618 still be a useful indicator of active vasculitis. In an analysis of 61 uveitic  
619 eyes (including a number with retinal vasculitis) and 94 healthy eyes  
620 Kim et al report that the superficial retinal plexus showed reduced  
621 parafoveal capillary density and reduced branching complexity in  
622 uveitic versus healthy eyes; vessel calibre was also not significantly  
623 different between uveitic and healthy eyes.<sup>84</sup>

624

625 ***Punctate inner chorioretinopathy (PIC)/ Multifocal choroiditis with***  
626 ***panuveitis (MCP) spectrum***

627 A significant challenge in the care of patients with PIC or multifocal  
628 choroiditis with panuveitis (MCP) is to distinguish whether new  
629 lesions are inflammatory, neovascular or both (Figure 9). This has  
630 major therapeutic implications. OCT findings may be very similar in  
631 both inflammatory lesions and CNV arising from the inner  
632 choroid/RPE with sub-RPE and subretinal involvement; although CNV  
633 may have greater heterogeneity than inflammatory lesions this is not  
634 always seen, and unlike some other types of CNV, they are not usually

635 associated with sub-retinal/sub-RPE fluid. Crucially both types of  
636 lesions may leak on FA. In a prospective case series of 17 eyes (12  
637 patients) with suspected active CNV in the context of PIC or MCP,  
638 Levison et al reported that OCTA was able to identify CNV features in  
639 15 eyes (11 patients).<sup>85</sup> They noted that identification was easier in the  
640 3x3mm rather than the 8x8mm scan. OCTA failed to identify the CNV in  
641 two eyes: in one, the CNV was a peripillary CNV; in the other, the CNV  
642 was obscured by a disciform scar with oedema. OCTA also provides a  
643 non-invasive way of monitoring the response to treatment (Figure 9).

644

645 OCTA may change our understanding of the risks of CNV formation in  
646 posterior uveitis. In a retrospective analysis of 18 eyes with multifocal  
647 choroiditis, Zahid et al reported that the majority of eyes (16/18) had  
648 lesions in which flow could be detected by OCTA, a much higher rate of  
649 neovascularization than previously reported in a series using other  
650 forms of imaging.<sup>86</sup> In a series of 40 eyes with multifocal choroiditis  
651 (26 patients), Cheng et al report that there were 23 active CNV cases  
652 detected on FA, of which 20 were confirmed on OCTA; the 3 which  
653 could not be confirmed had been excluded due to artefact.<sup>87</sup> The  
654 authors also imaged 34 lesions (13 eyes), which were thought to be

655 purely inflammatory, and noted that two of these showed flow on  
656 OCTA.<sup>87</sup>

657

658 Overall OCTA would suggest that the prevalence of unrecognised  
659 neovascularisation is high in these forms of uveitis. This may have  
660 implications for treatment, such a lower threshold for treatment with  
661 anti-VEGF therapy. Furthermore these new revelations may also have  
662 relevance to some of the more acute inflammatory syndromes, which  
663 are even less commonly thought to be associated with CNV. Chen et al  
664 report on four cases of atypical MEWDS who were all noted to have  
665 type 2 neovascularization on FA and/or OCTA.<sup>88</sup> It is likely that ready  
666 access to non-invasive angiographic assessment will reveal greater  
667 prevalence of neovascular elements in these conditions also. It is  
668 however noted that most of these cases do not progress to clinically  
669 visible CNV suggesting that a significant proportion do involute, either  
670 spontaneously or in response to immunosuppressive therapy.

671

### 672 ***Birdshot uveitis***

673 In a study of OCTA findings in eight eyes (four patients) with Birdshot  
674 Chorioretinopathy (BCR), de Carlo et al reported that all eyes showed

675 abnormalities including areas of reduced choroidal blood flow below  
676 the disrupted RPE, retinal thinning, abnormal telangiectatic vessels  
677 and an increased capillary space; the increased capillary space was  
678 most prominent temporally.<sup>89</sup> Additionally, capillary dilatations and  
679 loops were seen in 7/8 eyes. It is worth noting that these features were  
680 present even when classic birdshot lesions were not visible on fundus  
681 photography. Roberts et al reported on 37 eyes (21 patients) with BCR  
682 vs a similar number of healthy controls, and noted that the capillary  
683 density of the full retina, and both the superficial capillary plexus and  
684 deep capillary plexus were reduced in BCR compared to the healthy  
685 controls.<sup>90</sup> Importantly visual acuity in the BCR group was associated  
686 with a reduced capillary density, whereas FAZ area did not appear to  
687 have an effect.

688

### 689 ***Behcet's Uveitis***

690 In a prospective comparative study of FA, SD-OCT and OCTA in  
691 Behcet's disease, Khairallah et al noted the additional value of OCTA in  
692 detecting vascular abnormalities in 25 patients (44 eyes) with Behcet's  
693 disease.<sup>91</sup> They reported that perifoveal microvascular changes were  
694 noted more commonly on OCTA versus FA (96% vs 59%), with specific

695 abnormalities including disrupted perifoveal capillary arcades, retinal  
696 capillary under-perfusion, and rarefied, dilated, or shunted capillaries.  
697 These abnormalities were more commonly seen in the deep than in the  
698 superficial capillary plexus. Key differences in the Behcet's group  
699 versus healthy controls, included increased FAZ area of the superficial  
700 and deep capillary plexi, with lower overall capillary vessel density in  
701 the deep capillary plexus.

702

### 703 ***Vogt-Koyanagi-Harada Disease***

704 Clinically the early chorioretinal findings of acute VKH and multifocal  
705 central serous chorioretinopathy (CSC) may be similar. In a study of  
706 24 patients (10 VKH, 14 CSC), Aggarwal et al evaluated the ability of  
707 OCTA to identify differences that might help distinguish these  
708 entities<sup>92</sup>. They noted that in VKH there appeared to be a true  
709 choriocapillaris flow void related to ischaemia; an important caution  
710 however is that they also noted some similar changes in the CSC group,  
711 which they ascribed to overlying SRF and PED. The elicitation of true  
712 versus artefactual flow voids will be critical to its diagnostic utility in  
713 this context.

714

715 ***Acute Posterior Multifocal Placoid Pigment Epitheliopathy***

716 ***(APMPPE)***

717 The pathogenesis of APMPPE has been a controversial area ever since  
718 its original description by Gass and his proposal that it primarily  
719 targeted the RPE. Subsequent dye-based angiography has suggested  
720 that it may be primarily a choroidal vasculitis focused on the  
721 choriocapillaris. The application of OCTA may help to elucidate this.

722

723 In their report Kinouchi et al described a single case of APMPPE, in  
724 which they noted that in the acute phase OCTA demonstrated dark  
725 areas with a lack of flow signals at the level of the choriocapillaris  
726 corresponding to the placoid lesions. They suggested that this was not  
727 likely to be simply due to 'blockage' by RPE oedema, as flow signals  
728 from the deeper choroid in these regions were still present. Similarly  
729 Salvatore et al described a single case of APMPPE in which OCTA  
730 suggested altered flow and non-perfusion in defined islands of  
731 choriocapillaris. In both cases progressive reperfusion and visual  
732 recovery occurred over time.

733

734 Interestingly in their retrospective case series of five patients with

735 APMMPPE, Heiferman et al noted that choriocapillaris flow  
736 abnormalities extended beyond the visible lesions but cautioned  
737 against over-interpretation of the apparent flow voids immediately  
738 underlying the acute lesions due to the potential 'blockage' effect<sup>93</sup>.  
739 They did note however that after the acute phase when visualisation of  
740 the choroid improves, residual vascular abnormalities could be seen.  
741 Their finding that these vascular abnormalities may occur outside of  
742 the areas of clinically defined involvement, may suggest that the  
743 disease process in APMMPPE is more extensive than currently  
744 appreciated<sup>93</sup>.

745

746

#### 747 ***Other Retinal Inflammatory Lesions***

748 OCTA may be used to identify the presence of neovascularisation in  
749 other inflammatory foci, such as isolated retinal or choroidal lesions  
750 commonly termed 'granulomata'. Pichi et al describe a case of active  
751 Bartonella, in which OCTA of a retinal granuloma illustrated a network  
752 of vessels with microvascular proliferation within the inflammatory  
753 lesion<sup>94</sup>. Follow-up OCTA was also able to show reduction of the  
754 vascular network as the lesion responded to treatment.<sup>94</sup>

755

756 **OCTA in Optic Nerve Disease**

757

758 ***Glaucoma***

759 Primary open angle glaucoma (POAG) is a multifactorial optic  
760 neuropathy, possibly involving vascular dysfunction, leading to death  
761 of retinal ganglion cells and of their axons. Exploration of ocular  
762 vasculature in glaucoma has been challenging, due to various  
763 limitations in the imaging modalities; therefore, the novel  
764 developments of OCTA have raised a large interest in exploring the  
765 optic nerve microvasculature in POAG. Initial, cross-sectional studies  
766 have suggested that OCTA can be useful in evaluating the optic disc and  
767 the peripapillary retinal perfusion in glaucoma.<sup>95,96</sup> Furthermore, these  
768 studies have shown the ability of OCTA to display attenuation of the  
769 optic nerve microvasculature in POAG, both at the optic nerve head  
770 level and at the peripapillary area, compared to normal eyes. Thus,  
771 OCTA allows non-invasive 3D visualization of the optic nerve head  
772 vasculature, from the disc surface to the lamina cribrosa, as well as  
773 quantification of optic disc perfusion.

774 Conventional OCT has successfully provided objective and quantitative

775 structural measurements in POAG, including evaluation of ganglion cell  
776 complex in the macular region and retinal nerve fiber layer (RNFL)  
777 thickness at peripapillary regions. However, these conventional  
778 structural OCT measurements do not seem to entirely reflect the  
779 functional outcome in glaucoma. Indeed, structural loss in glaucoma  
780 has only moderate correlation with loss of the visual field (VF) in  
781 POAG, especially at early stages. On the contrary OCTA not only reveals  
782 reduced retinal vessel density in POAG, but OCTA findings also  
783 correlate well with the disease severity and the associated visual field  
784 loss.<sup>97</sup> These significant vascular-functional correlations in POAG,  
785 revealed by OCTA, might be explained by a pre-apoptotic status of the  
786 retinal ganglion cells at early stages. These cells and their axons may  
787 be affected only functionally at the early stages, due to the reduced  
788 vascular supply (as shown by OCTA). Their subsequent damage may  
789 translate only later into reduced visual field sensitivity and OCTA may  
790 allow the early detection of microvascular abnormalities in the course  
791 of POAG. Indeed, OCTA can disclose decreased peripapillary, optic  
792 nerve head and macular vessel densities, not only in early glaucoma  
793 with limited VF loss, but also in pre-perimetric POAG, when standard  
794 automated perimetry is still intact, despite RNFL thinning.<sup>98</sup> OCTA may

795 also be helpful for exploring vascular changes in secondary optic  
796 glaucomatous optic neuropathies due to neuro-ophthalmic conditions,  
797 such as increased episcleral vessels pressure occurring in carotid-  
798 cavernous fistulas.<sup>99</sup>

799

800 Taken together, these initial cross-sectional, observational studies  
801 suggest that OCTA may represent a potential tool for detecting  
802 vascular abnormalities in POAG, which may translate in the future into  
803 early diagnosis and improved disease monitoring. However, these  
804 preliminary studies have several inherent (technical, methodological)  
805 limitations and most importantly, do not explain yet if the  
806 microvascular attenuation in POAG is a cause or rather a consequence  
807 of the glaucomatous condition. Longitudinal studies may clarify in the  
808 future this complex temporal relationship.

809

### 810 ***Non-arteritic ischemic optic neuropathy***

811 Non-arteritic anterior ischemic optic neuropathy (NAION), the most  
812 common non-glaucomatous optic neuropathy in the elderly  
813 population, is characterized by acute, painless, typically unilateral  
814 visual loss and altitudinal visual field defect, associated with optic disc

815 swelling. NAION is possibly caused by transient hypoperfusion in the  
816 capillary bed of the optic nerve head, which is closely connected with  
817 the choroidal vasculature – explaining the high interest of its  
818 exploration with OCTA.

819 OCTA may allow evaluation of the peripapillary microvasculature in  
820 eyes with NAION, both at the acute stage (Figure 10), and after  
821 resolution of the optic disc swelling.<sup>100</sup> In a small pilot study, exploring  
822 eyes with NAION at the acute stage (within 1 week of visual loss),  
823 OCTA imaging revealed significant segmental and global reduction of  
824 the peripapillary vascular flow density, compared to the fellow, healthy  
825 eyes and to age-matched control eyes. In addition, OCTA may also  
826 reveal tortuous capillaries within or surrounding the optic disc in  
827 NAION, a finding clinically described as pseudoangiomatous  
828 hyperplasia<sup>101</sup>. It is not clear yet if OCTA may be useful for the  
829 longitudinal follow-up in NAION, but preliminary data suggests that  
830 OCTA may reveal spontaneous, partial recovery of peripapillary  
831 vascular flow densities during the natural course of the disease, in line  
832 with the limited improvement of the visual function.<sup>100</sup> In addition,  
833 OCTA may also have the ability to evaluate progression of the disease,  
834 i.e. from an infra-clinical, incipient stage of NAION to its full-blown

835 clinical picture.<sup>100</sup> OCTA may therefore have a potential role in  
836 monitoring the evolution of NAION.

837

838 However, OCTA has specific limitations in the evaluation of NAION. The  
839 reduction of the flow density at different layers in NAION may not  
840 reflect a primary ischemic process, but rather may be the result of  
841 compressive oedema, or of imaging artefacts (signal attenuation by  
842 blood and/or oedema).

843

844 ***Optic neuritis, multiple sclerosis and optic atrophy***

845 OCTA has been used for the evaluation of the optic nerve head  
846 microvasculature in other neuro-ophthalmic conditions causing either  
847 true or pseudo-optic disc oedema (idiopathic intracranial  
848 hypertension, Leber's hereditary optic neuropathy) or, at later stages,  
849 optic disc atrophy (after optic neuritis, NAION, or in autosomal  
850 dominant optic atrophy).<sup>101</sup> Optic disc oedema, irrespective of its  
851 origin, may be associated with vessel tortuosity and dilated prelaminar  
852 capillary network on OCTA, but the magnitude of the associated  
853 vascular dropout may depend on the nature of the optic nerve  
854 condition and its severity. Optic disc oedema related to idiopathic

855 intracranial hypertension may be associated with relatively preserved  
856 peripapillary microvasculature in its early stages (Figure 2). Further  
857 longitudinal studies are needed to assess the natural history of OCTA  
858 findings in optic disc oedema.

859 Patients with multiple sclerosis (MS) who had previous episodes of  
860 optic neuritis display a reduced peripapillary and parafoveal vascular  
861 flow index, compared to healthy controls, as well as compared to  
862 patients with MS without previous optic neuritis attacks.<sup>102,103</sup>

863 Interestingly, even in absence of optic neuritis attacks, patients with  
864 defined MS display a reduced vascular flow with OCTA, compared to  
865 controls.<sup>102,103</sup> In patients with optic neuritis, OCTA may display  
866 residual microvascular abnormalities of the optic nerve and the  
867 macula, despite recovery of visual function after treatment.<sup>103</sup>

868

### 869 **OCTA in Anterior Segment Disease**

870

871 Angiography for the anterior segment has a variety of clinical  
872 applications, ranging from the evaluation of scleral inflammatory  
873 disorders, to the assessment of corneal vascularization. Currently, the  
874 assessment of the anterior segment vasculature is constrained to

875 invasive angiography techniques using FA or ICGA. However, invasive  
876 angiography techniques expose patients to potential adverse reactions.  
877 Thus, imaging and evaluation of corneal vascularization has been  
878 limited, despite its prevalence and potential sight-threatening effects.  
879 Also, significant time and preparation is required before each ICGA or  
880 FA imaging session, while some patients may not be suitable for this  
881 procedure at all, due to various contraindications. Thus there is an  
882 increasing role for OCTA for the anterior segment<sup>104</sup>.

883

884 The main advantage of OCTA for the anterior segment is that images  
885 are rapidly acquired using a non-contact technique.<sup>105</sup> While the split-  
886 spectrum amplitude-decorrelation angiography (SSADA) system has  
887 been most commonly described for the anterior segment, other  
888 spectral domain and swept source OCTA systems have also been  
889 successfully adapted for the anterior segment.<sup>106</sup> However, it is  
890 important to note that current OCTA systems are not specifically  
891 designed for the anterior segment but may be adapted to assess the  
892 cornea or iris vasculature.<sup>105</sup> Thus there are several limitations such as  
893 the inability to demonstrate vessel leakage, and a limited field of view  
894 compared to the FA and ICGA.<sup>107</sup> Moreover, as the lens had to be

895 relatively close to the surface of the cornea for the vessels to be in  
896 focus, image acquisition was relatively easier in the temporal  
897 quadrants compared to the nasal scans. Nonetheless, it has been  
898 reported that the OCTA adapted for the cornea was comparable to  
899 ICGA for measurement of the area of corneal vascularization in one  
900 pilot clinical study.<sup>108</sup>

901

902 Similar to the OCTA for the retina and posterior segment, there are  
903 several points to note when interpreting OCTA scans for the anterior  
904 segment. First, image distortions may occur due to patient movement,  
905 inclinations of the scanning plane relative due to the corneal surface.  
906 Fortunately, as each non-contact scan only requires 3-4 seconds to  
907 complete, patients are usually able to tolerate multiple scans to ensure  
908 a good quality image is achieved. Second, image artefacts and loss of  
909 signal may occur in areas of dense scarring, and be compounded by the  
910 coronal reconstruction of scans. Future improvements to the software  
911 and optimization for the anterior segment may further improve the  
912 image resolution, before which a clinician may choose to perform ICGA  
913 in eyes with concomitant dense corneal scarring. Third, the OCTA  
914 systems for the anterior segment used do not come with an in-built

915 motion correction for ocular saccades or micro-movements. It also  
916 does not carry an eye-tracking system with registration, which is  
917 required for comparisons in follow-up scans. Nonetheless, with the  
918 help of adjunct image analysis software, it has been found to be  
919 potentially useful for serial scans and follow-up in various clinical  
920 indications.

921

922 While recognizing the current limitations of OCTA systems, there are  
923 still a wide variety of potential clinical applications for delineating the  
924 vasculature of the anterior segment (Figure 11).<sup>99</sup> These include  
925 assessment of graft vascularization with prognostication for graft  
926 rejection, evaluation of new anti-angiogenic treatments for corneal  
927 vascularization, studying limbal vasculature associated with limbal  
928 stem cell deficiency, or even evaluation of bleb vascularity and  
929 morphology after glaucoma surgery (Figure 11). The ability to provide  
930 high-resolution scans of the cornea with accompanying information on  
931 the depth of abnormal vasculature, is useful for planning for  
932 procedures such as lamellar keratoplasty and fine-needle diathermy;  
933 or evaluation of peripheral corneal infiltrates or melts with the  
934 adjacent inflamed sclera and limbal vessels. Moreover, while the

935 presence of FA or ICGA leakage influences clinical management for  
936 retinal or choroidal pathology, in the anterior segment leakage blocks  
937 vessel delineation and adds limited clinical information. On the other  
938 hand, the absence of vascular flow may be a more useful clinical sign,  
939 for example in the assessment of peripheral ulcerative keratitis, a sign  
940 which is often obscured by the leakage or extravasation of dye. The  
941 progression of corneal melting and the need for systemic  
942 immunosuppression in such severe inflammatory conditions is usually  
943 preceded by vasculitis and vaso-occlusion of the limbal vessels; while  
944 recanalization and new capillary formation may indicate response to  
945 treatment. Thus, OCTA has the potential to play an important role in  
946 detecting progression, prognostication and the management of these  
947 corneoscleral destructive diseases, which requires further studies in  
948 these specific conditions for confirmation.

949

#### 950 **Other novel areas of interest**

951

952 Other upcoming applications of OCTA include the visualisation of the  
953 middle retinal plexus, the peri-papillary radial plexus as well as  
954 changes within the choriocapillaris and large choroidal vessels,

955 previously not adequately visualized using conventional angiography;  
956 however the clinical significance of changes is unclear. The  
957 development of variable inter-scan time acquisition protocols (VISTA)  
958 may also allow variable flow rates (both slow and fast) to be detected  
959 in future OCTA platforms<sup>109</sup>.

960

## 961 **Summary**

962

963 Optical coherence tomography angiography (OCTA) has emerged as a  
964 novel, non-invasive imaging modality that allows the detailed study of  
965 flow within the vascular structures of the eye. This new technology,  
966 still in its infancy, has the potential to improve the diagnosis and  
967 monitoring of various vascular and inflammatory diseases by imaging  
968 vascular networks in greater detail than ever before. In addition, to the  
969 retina, OCTA can be used also in the anterior segment and optic nerve.  
970 Keeping in mind the current limitations of this technology, future  
971 technical improvements and increased validation of this promising  
972 imaging modality is necessary to improve the clinical application of  
973 OCTA.

974 **Legends**

975

976 **Figure 1: OCTA of a single normal eye showing variations in the**  
977 **scan area and algorithms.** *Cross sectional OCTA images of the*  
978 *superficial vascular plexus segmentation (top row) and deep vascular*  
979 *plexus (third row). En face OCTA images of the superficial vascular*  
980 *plexus segmentation (second row) and deep vascular plexus (bottom*  
981 *row). A: An 8x8 mm scan taken with the AngioVue RTVue XR Avanti*  
982 *processed with the SADA algorithm; B: A 6x6 mm scan taken with the*  
983 *Angioplex CIRRUS HD-OCT Model 5000 processed with the OMAG*  
984 *algorithm; C: A 3x3 mm scan taken with DRI-OCT Triton swept source*  
985 *OCT processed with the OCTA-RA algorithm. On the automated*  
986 *segmentation of the deep vascular plexus of both the Angiovue and*  
987 *Angioplex, some projection artefact from the superficial layer is*  
988 *observed.*

989

990 **Figure 2: A summary of an approach to OCTA interpretation.**

991

992 **Figure 3: Examples of common artefacts seen on OCTA.** *A: Motion*  
993 *artefact seen by black vertical lines caused by blinking (yellow*

994 arrowhead) and eye movements (green arrowhead). B: An example of a  
995 projection artefact (yellow boxes) of the superficial vessels seen in the  
996 deep vascular plexus segmentation. Comparing the deep vascular plexus  
997 segmentation, all the projection artefact seen can be accounted for by  
998 the more superficial vessels (green boxes). C: Unmasking artefact seen as  
999 an area of high flow (middle of crosshairs) on en face OCTA (left), cross-  
1000 sectional OCTA (middle) showed a focal area of atrophy with underlying  
1001 hyper-transmission of the signal (yellow arrow). Area of high flow on en  
1002 face OCTA can be accounted for by an area of atrophy causing the  
1003 underlying choroidal vessels to be seen as an area of unmasking artefact.  
1004 This is confirmed by the corresponding area of hypo-autofluorescence  
1005 seen on fundus autofluorescence (right). D: Enface OCTA (left)  
1006 corresponding to cross sectional OCTA (middle top) showing a straight  
1007 segmentation line that does not capture polyps (blue arrow) seen at the  
1008 peak of the pigment epithelial detachment. Alternatively, when using the  
1009 RPE fit segmentation the area of polyps (orange arrow) are then seen on  
1010 en face OCTA

1011

1012 **Figure 4: Multimodal images including OCTA images of the 3**  
1013 **subtypes of neovascular age-related macular degeneration.**

1014 *(CFP=colour fundus photo, FA=fundus fluorescein angiography,*  
1015 *ICGA=indocyanine green angiography, OCTA= topical coherence*  
1016 *tomography angiography, OCT= optical coherence tomography) A: Type*  
1017 *1 neovascularisation (NV) (yellow arrows) with a vascularised pigment*  
1018 *epithelial detachment seen on CFP, stippled hyperfluorescence and late*  
1019 *leakage on FA, a plaque on ICGA and a vascular network seen on en face*  
1020 *OCTA with a corresponding area of abnormal flow seen under the RPE on*  
1021 *cross sectional OCTA. B: Type 2 NV (green arrows) with a greyish*  
1022 *membrane seen on CFP, early lacy hyperfluorescence with late leakage*  
1023 *seen on FA and a vascular network seen on en face OCTA with abnormal*  
1024 *flow seen above the RPE on cross-sectional OCTA. C: Type 3 NV (blue*  
1025 *arrows) seen with associated atrophy on CFP, pinpoint leakage on FA*  
1026 *with an area of abnormal flow on en face OCTA corresponding to a linear*  
1027 *area of abnormal flow in the deep retina seen on cross-sectional OCTA*  
1028 *seen below a large patch of geographic atrophy.*

1029

1030 ***Figure 5: Multimodal images including OCTA images of mixed***  
1031 ***subtypes of neovascular age-related macular degeneration.***

1032 *(CFP=colour fundus photo, FAF= fundus autofluorescence, FA=fundus*

1033 *fluorescein angiography, ICGA=indocyanine green angiography, OCTA=*

1034 *topical coherence tomography angiography, OCT= optical coherence*  
1035 *tomography). A: Type 1 neovascularisation (NV) with polypoidal*  
1036 *choroidal vasculopathy. Polyps (blue arrows) seen as orange nodules on*  
1037 *CFP, focal leakage on FA, clusters of hypercyanescence on ICGA and a*  
1038 *focal area of increased flow surrounded by a halo of decreased flow*  
1039 *signal on en face OCTA with a corresponding area of abnormal flow*  
1040 *directly under the RPE seen on cross sectional OCTA. An associated*  
1041 *branching vascular network or type 1 NV (orange arrows) seen as*  
1042 *stippled hyperfluorescence on FA, a plaque on ICGA and a vascular*  
1043 *network on OCTA corresponding to shallow, irregular pigment epithelial*  
1044 *detachment containing abnormal flow seen on cross sectional OCTA. B: A*  
1045 *mixed type 2 and type 1 NV with the subretinal type 2 component (yellow*  
1046 *circles and arrow) and the sub-retinal pigment epithelial type 1*  
1047 *component (green circles and arrows).*

1048

1049 ***Figure 6: OCTA images showing different neovascularisation (NV)***  
1050 ***responses to treatment with intravitreal anti-vascular endothelial***  
1051 ***growth factor therapy (IVT). A: En face OCTA (top row) shows after 1***  
1052 ***IVT, there is reduction in the overall size of the type 2 NV with the***  
1053 ***regression of the smaller peripheral anastomosis leaving the larger***

1054 calibre vessel trunks. After 3 IVTs the lesion size remains stable with the  
1055 persistence of the larger calibre vessel trunks with a reduction in the  
1056 dark halo surrounding the vascular lesion. Corresponding cross-sectional  
1057 OCTA (second row) that show the reduction in the area of abnormal flow  
1058 (red overlay) during the course of treatment. B: Enface OCTA with color-  
1059 coded density mapping showing the reduction in size of the type 1 NV  
1060 (red) from baseline and after 6 IVTs with corresponding cross-sectional  
1061 OCTAs showing a reduction in abnormal flow (red overlay) from  
1062 baseline.

1063

1064 **Figure 7: OCTA features in diabetic retinopathy.** A: An eye with severe  
1065 non-proliferative diabetic retinopathy with microaneurysms  
1066 surrounding the fovea as seen on fluorescein angiography (left) and the  
1067 corresponding 6x6 (middle) and 3x3 (right) en face OCTA of the  
1068 superficial segmentation. An enlarged foveal avascular zone (FAZ) is also  
1069 noted (yellow arrows). B: An eye with diabetic macula oedema and an  
1070 enlarged FAZ (green arrow) with disruption of the normal vasculature  
1071 inferiorly as seen on enface OCTA with superficial segmentation (left)  
1072 and corresponding cross-sectional OCTA middle (top) and similarly with  
1073 deep segmentation (right and middle bottom). Both the cystic spaces

1074 *from diabetic macula oedema and areas of non-perfusion are seen as*  
1075 *dark areas on the deep segmentation en face OCTA.*

1076

1077 **Figure 8: OCTA features of branch retinal vein occlusion.** *A: Fundus*  
1078 *fluorescein angiography (FA) showing an ischaemic branch retinal vein*  
1079 *occlusion with neovascularisation and areas of capillary non-perfusion.*  
1080 *B: The areas of non-perfusion corresponding to the FA (yellow box) are*  
1081 *seen clearly on en face OCTA. C: An area of neovascularisation leaking on*  
1082 *FA (green box) is seen on en face OCTA as a small vascular tuft of high*  
1083 *flow growing into the posterior hyaloid as seen on cross sectional OCTA.*

1084

1085 **Figure 9: OCTA identifies neovascular membrane secondary to**  
1086 **punctate inner chorioretinopathy (PIC).** *A: En face OCTA shows an area*  
1087 *of absent flow (yellow circle) on the choriocapillary segmentation seen to*  
1088 *correspond with a hyper-reflective inflammatory lesion (yellow arrow)*  
1089 *on cross sectional OCTA with absent flow. B: Another PIC lesion seen on*  
1090 *colour fundus photo (top left), the corresponding en face OCTA shows a*  
1091 *secondary choroidal neovascularisation (CNV) (blue circle), with the*  
1092 *corresponding cross sectional OCTA showing an area of abnormal flow*  
1093 *(blue arrow) on the hyper-reflective inflammatory lesion. After 1*

1094 *intravitreal anti-vascular endothelial growth factor therapy (IVT)*  
1095 *(bottom row), there is regression of the CNV seen on both en face and*  
1096 *cross sectional OCTA (blue circle and arrow).*

1097

1098 **Figure 10. OCTA findings in a patient with non-arteritic ischemic**  
1099 **optic neuropathy and ipsilateral visual loss.** *The sectorial optic disc*  
1100 *swelling (A), is associated on OCTA (AngioVue, Optovue) with tortuous*  
1101 *radial peripapillary capillaries and vascular dropout in the optic nerve*  
1102 *head (B). Optic nerve head swelling in a patient with idiopathic*  
1103 *intracranial hypertension and preserved visual function (C). Despite the*  
1104 *severe optic disc swelling and peripapillary hemorrhages (C), OCTA*  
1105 *evaluation (AngioVue, Optovue), discloses only limited vascular dropout*  
1106 *in the optic nerve head region (D & E).*

1107

1108 **Figure 11. Optical coherence tomography angiography of the**  
1109 **cornea.** *A. Fungal keratitis with chronic inflammation and corneal*  
1110 *vascularisation. B. Optical coherence tomography angiography imaging*  
1111 *may be useful to guide fine needle diathermy and anti-VEGF therapy to*  
1112 *reduce corneal vascularisation before corneal transplantation, and risk*  
1113 *of corneal graft rejection. C. Interstitial keratitis with deep corneal*

1114 *vascularisation. D. Optical coherence tomography angiography reveals*  
1115 *deeper vessels not obvious on slit-lamp microscopy.*

1116

1117

1118 ***Table 1: Comparison of optical coherence tomography angiography***  
1119 ***(OCTA) versus conventional angiography such as fundus fluorescein***  
1120 ***angiography (FA) and indocyanine green angiography (ICGA).***

1121

1122 ***Table 2: Comparison of four current commercially available optical***  
1123 ***coherence tomography angiography (OCTA) platforms and their various***  
1124 ***specifications (Information up to date as of January 2017).***

1125

1126 ***Table 3: Multimodal characteristics of atrophic age-related macular***  
1127 ***degeneration (AMD) and subtypes of neovascular AMD***

1128

1129

1130

1131 ***Acknowledgments:***

1132

1133 *Dr Raymond Najjar and Dr Sourabh Sharma for help with the figures.*

1134

1135 **Financial disclosures:** ACT is a consultant for Zeiss and has received  
1136 travel grants and sponsorship from Bayer, Allergan and Mandarin Optics.  
1137 GT is a consultant for Novartis and Abbott medical, a speaker and receives  
1138 travel support from Allergan, Alcon, Zeiss and Bayer; in addition to grant  
1139 and travel support from Santen. AKD receive a proportion of their funding  
1140 from the National Institute for Health Research (NIHR) Biomedical  
1141 Research Centre based at Moorfields Eye Hospital NHS Foundation Trust  
1142 and UCL Institute of Ophthalmology. PAK is funded by a Clinician  
1143 Scientist award (CS-2014-14-023) from the National Institute for Health  
1144 Research. The views expressed in this publication are those of the authors  
1145 and not necessarily those of the NHS, the National Institute for Health  
1146 Research or the Department of Health. PAK has received speaker fees from  
1147 Heidelberg Engineering, Topcon, Haag-Streit, Allergan, Novartis, and  
1148 Bayer. He has served on advisory boards for Novartis and Bayer, and is an  
1149 external consultant for DeepMind and Optos. UC receives grant funding  
1150 from Alimera Sciences, lectures and speaking events for Allergan. GC is a  
1151 consultant, speaker and receives grant funding from Novartis and Bayer, is  
1152 also a speaker for Allergan and Topcon. The remaining authors have no  
1153 conflicting interests to disclose.

1154

1155

1156   **REFERENCES**

- 1157   1.    Gao SS, Jia Y, Zhang M, et al. Optical Coherence Tomography Angiography.  
1158       *Investigative ophthalmology & visual science*. 2016;57(9):OCT27-36.
- 1159   2.    Zhang A, Zhang Q, Chen CL, Wang RK. Methods and algorithms for optical  
1160       coherence tomography-based angiography: a review and comparison. *Journal of*  
1161       *biomedical optics*. 2015;20(10):100901.
- 1162   3.    Jia Y, Bailey ST, Wilson DJ, et al. Quantitative optical coherence tomography  
1163       angiography of choroidal neovascularization in age-related macular degeneration.  
1164       *Ophthalmology*. 2014;121(7):1435-1444.
- 1165   4.    Kuehlewein L, Sadda SR, Sarraf D. OCT angiography and sequential quantitative  
1166       analysis of type 2 neovascularization after ranibizumab therapy. *Eye (Lond)*.  
1167       2015;29(7):932-935.
- 1168   5.    Tan AC, Dansingani KK, Yannuzzi LA, Sarraf D, Freund KB. Type 3  
1169       Neovascularization Imaged with Cross-Sectional and En Face Optical Coherence  
1170       Tomography Angiography. *Retina*. 2017;37(2):234-246.
- 1171   6.    Phasukkijwatana N, Tan AC, Chen X, Freund KB, Sarraf D. Optical coherence  
1172       tomography angiography of type 3 neovascularisation in age-related macular  
1173       degeneration after antiangiogenic therapy. *The British journal of ophthalmology*.  
1174       2016.
- 1175   7.    Lumbroso B, Rispoli M, Savastano MC. Longitudinal Optical Coherence  
1176       Tomography-Angiography Study of Type 2 Naive Choroidal Neovascularization  
1177       Early Response after Treatment. *Retina*. 2015;35(11):2242-2251.
- 1178   8.    Ferrara D. Image artifacts in optical coherence tomography angiography. *Clinical*  
1179       *& experimental ophthalmology*. 2016;44(5):367-368.
- 1180   9.    Spaide RF, Fujimoto JG, Waheed NK. Image Artifacts in Optical Coherence  
1181       Tomography Angiography. *Retina*. 2015;35(11):2163-2180.
- 1182   10.   Kraus MF, Liu JJ, Schottenhamml J, et al. Quantitative 3D-OCT motion correction  
1183       with tilt and illumination correction, robust similarity measure and  
1184       regularization. *Biomedical optics express*. 2014;5(8):2591-2613.
- 1185   11.   Camino A, Zhang M, Gao SS, et al. Evaluation of artifact reduction in optical  
1186       coherence tomography angiography with real-time tracking and motion  
1187       correction technology. *Biomedical optics express*. 2016;7(10):3905-3915.
- 1188   12.   Coscas G, Lupidi M, Coscas F. Image Analysis of Optical Coherence Tomography  
1189       Angiography. *Developments in ophthalmology*. 2016;56:30-36.
- 1190   13.   Chen FK, Viljoen RD, Bukowska DM. Classification of image artefacts in optical  
1191       coherence tomography angiography of the choroid in macular diseases. *Clinical &*  
1192       *experimental ophthalmology*. 2016;44(5):388-399.
- 1193   14.   Huang Y, Zhang Q, Wang RK. Efficient method to suppress artifacts caused by  
1194       tissue hyper-reflections in optical microangiography of retina in vivo. *Biomedical*  
1195       *optics express*. 2015;6(4):1195-1208.
- 1196   15.   Dansingani KK, Tan AC, Gilani F, et al. Subretinal Hyperreflective Material Imaged  
1197       With Optical Coherence Tomography Angiography. *Am J Ophthalmol*.  
1198       2016;169:235-248.
- 1199   16.   Malihi M, Jia Y, Gao SS, et al. Optical coherence tomographic angiography of  
1200       choroidal neovascularization ill-defined with fluorescein angiography. *The British*  
1201       *journal of ophthalmology*. 2017;101(1):45-50.

- 1202 17. Tan AC, Simhaee D, Balaratnasingam C, Dansingani KK, Yannuzzi LA. A  
1203 Perspective on the Nature and Frequency of Pigment Epithelial Detachments. *Am J*  
1204 *Ophthalmol.* 2016;172:13-27.
- 1205 18. Kuehlewein L, Bansal M, Lenis TL, et al. Optical Coherence Tomography  
1206 Angiography of Type 1 Neovascularization in Age-Related Macular Degeneration.  
1207 *Am J Ophthalmol.* 2015;160(4):739-748.e732.
- 1208 19. Inoue M, Jung JJ, Balaratnasingam C, et al. A Comparison Between Optical  
1209 Coherence Tomography Angiography and Fluorescein Angiography for the  
1210 Imaging of Type 1 Neovascularization. *Invest Ophthalmol Vis Sci.*  
1211 2016;57(9):OCT314-323.
- 1212 20. Veronese C, Maiolo C, Morara M, Armstrong GW, Ciardella AP. Optical Coherence  
1213 Tomography Angiography to Assess Pigment Epithelial Detachment. *Retina.*  
1214 2016;36(3):645-650.
- 1215 21. Costanzo E, Miere A, Querques G, Capuano V, Jung C, Souied EH. Type 1 Choroidal  
1216 Neovascularization Lesion Size: Indocyanine Green Angiography Versus Optical  
1217 Coherence Tomography Angiography. *Invest Ophthalmol Vis Sci.*  
1218 2016;57(9):OCT307-313.
- 1219 22. El Ameen A, Cohen SY, Semoun O, et al. Type 2 Neovascularization Secondary to  
1220 Age-Related Macular Degeneration Imaged by Optical Coherence Tomography  
1221 Angiography. *Retina.* 2015;35(11):2212-2218.
- 1222 23. Coscas G, Lupidi M, Coscas F, Francais C, Cagini C, Souied EH. Optical coherence  
1223 tomography angiography during follow-up: qualitative and quantitative analysis  
1224 of mixed type I and II choroidal neovascularization after vascular endothelial  
1225 growth factor trap therapy. *Ophthalmic research.* 2015;54(2):57-63.
- 1226 24. Tan AC, Dansingani KK, Yannuzzi LA, Sarraf D, Freund KB. Type 3  
1227 Neovascularization Imaged with Cross-Sectional and En Face Optical Coherence  
1228 Tomography Angiography. *Retina.* 2016.
- 1229 25. Kuehlewein L, Dansingani KK, de Carlo TE, et al. Optical Coherence Tomography  
1230 Angiography of Type 3 Neovascularization Secondary to Age-Related Macular  
1231 Degeneration. *Retina.* 2015;35(11):2229-2235.
- 1232 26. Tsai AS, Cheung N, Gan AT, et al. Retinal Angiomatous Proliferation. *Survey of*  
1233 *ophthalmology.* 2017.
- 1234 27. Coscas GJ, Lupidi M, Coscas F, Cagini C, Souied EH. OPTICAL COHERENCE  
1235 TOMOGRAPHY ANGIOGRAPHY VERSUS TRADITIONAL MULTIMODAL IMAGING  
1236 IN ASSESSING THE ACTIVITY OF EXUDATIVE AGE-RELATED MACULAR  
1237 DEGENERATION: A New Diagnostic Challenge. *Retina.* 2015;35(11):2219-2228.
- 1238 28. Marques JP, Costa JF, Marques M, Cachulo ML, Figueira J, Silva R. Sequential  
1239 Morphological Changes in the CNV Net after Intravitreal Anti-VEGF Evaluated  
1240 with OCT Angiography. *Ophthalmic research.* 2016;55(3):145-151.
- 1241 29. Muakkassa NW, Chin AT, de Carlo T, et al. Characterizing the Effect of Anti-  
1242 Vascular Endothelial Growth Factor Therapy on Treatment-Naive Choroidal  
1243 Neovascularization Using Optical Coherence Tomography Angiography. *Retina.*  
1244 2015;35(11):2252-2259.
- 1245 30. Spaide RF. Optical Coherence Tomography Angiography Signs of Vascular  
1246 Abnormalization With Antiangiogenic Therapy for Choroidal Neovascularization.  
1247 *American journal of ophthalmology.* 2015;160(1):6-16.
- 1248 31. Inoue M, Balaratnasingam C, Freund KB. Optical Coherence Tomography  
1249 Angiography of Polypoidal Choroidal Vasculopathy and Polypoidal Choroidal  
1250 Neovascularization. *Retina.* 2015;35(11):2265-2274.

- 1251 32. Tomiyasu T, Nozaki M, Yoshida M, Ogura Y. Characteristics of Polypoidal  
1252 Choroidal Vasculopathy Evaluated by Optical Coherence Tomography  
1253 Angiography. *Investigative ophthalmology & visual science*. 2016;57(9):OCT324-  
1254 330.
- 1255 33. Tanaka K, Mori R, Kawamura A, Nakashizuka H, Wakatsuki Y, Yuzawa M.  
1256 Comparison of OCT angiography and indocyanine green angiographic findings  
1257 with subtypes of polypoidal choroidal vasculopathy. *The British journal of*  
1258 *ophthalmology*. 2017;101(1):51-55.
- 1259 34. Cheung CM, Yanagi Y, Mohla A, et al. Characterization and Differentiation of  
1260 Polypoidal Choroidal Vasculopathy Using Swept Source Optical Coherence  
1261 Tomography Angiography. *Retina*. 2016.
- 1262 35. Wang M, Zhou Y, Gao SS, et al. Evaluating Polypoidal Choroidal Vasculopathy With  
1263 Optical Coherence Tomography Angiography. *Investigative ophthalmology &*  
1264 *visual science*. 2016;57(9):OCT526-532.
- 1265 36. Srouf M, Querques G, Semoun O, et al. Optical coherence tomography angiography  
1266 characteristics of polypoidal choroidal vasculopathy. *The British journal of*  
1267 *ophthalmology*. 2016.
- 1268 37. Takayama K, Ito Y, Kaneko H, et al. Comparison of indocyanine green angiography  
1269 and optical coherence tomographic angiography in polypoidal choroidal  
1270 vasculopathy. *Eye*. 2017;31(1):45-52.
- 1271 38. Miere A, Semoun O, Cohen SY, et al. Optical Coherence Tomography Angiography  
1272 Features of Subretinal Fibrosis in Age-Related Macular Degeneration. *Retina*.  
1273 2015;35(11):2275-2284.
- 1274 39. Dansingani KK, Balaratnasingam C, Klufas MA, Sarraf D, Freund KB. Optical  
1275 coherence tomography angiography of shallow irregular pigment epithelial  
1276 detachments in pachychoroid spectrum disease. *Am J Ophthalmol*. 2015.
- 1277 40. Dansingani KK, Balaratnasingam C, Klufas MA, Sarraf D, Freund KB. Optical  
1278 Coherence Tomography Angiography of Shallow Irregular Pigment Epithelial  
1279 Detachments In Pachychoroid Spectrum Disease. *American journal of*  
1280 *ophthalmology*. 2015;160(6):1243-1254 e1242.
- 1281 41. Carnevali A, Cicinelli MV, Capuano V, et al. Optical Coherence Tomography  
1282 Angiography: A Useful Tool for Diagnosis of Treatment-Naive Quiescent Choroidal  
1283 Neovascularization. *Am J Ophthalmol*. 2016;169:189-198.
- 1284 42. Roisman L, Zhang Q, Wang RK, et al. Optical Coherence Tomography Angiography  
1285 of Asymptomatic Neovascularization in Intermediate Age-Related Macular  
1286 Degeneration. *Ophthalmology*. 2016;123(6):1309-1319.
- 1287 43. Palejwala NV, Jia Y, Gao SS, et al. DETECTION OF NONEXUDATIVE CHOROIDAL  
1288 NEOVASCULARIZATION IN AGE-RELATED MACULAR DEGENERATION WITH  
1289 OPTICAL COHERENCE TOMOGRAPHY ANGIOGRAPHY. *Retina*. 2015;35(11):2204-  
1290 2211.
- 1291 44. Waheed NK, Moulton EM, Fujimoto JG, Rosenfeld PJ. Optical Coherence Tomography  
1292 Angiography of Dry Age-Related Macular Degeneration. *Developments in*  
1293 *ophthalmology*. 2016;56:91-100.
- 1294 45. Moulton EM, Waheed NK, Novais EA, et al. Swept-Source Optical Coherence  
1295 Tomography Angiography Reveals Choriocapillaris Alterations in Eyes with  
1296 Nascent Geographic Atrophy and Drusen-Associated Geographic Atrophy. *Retina*.  
1297 2016;36 Suppl 1:S2-S11.

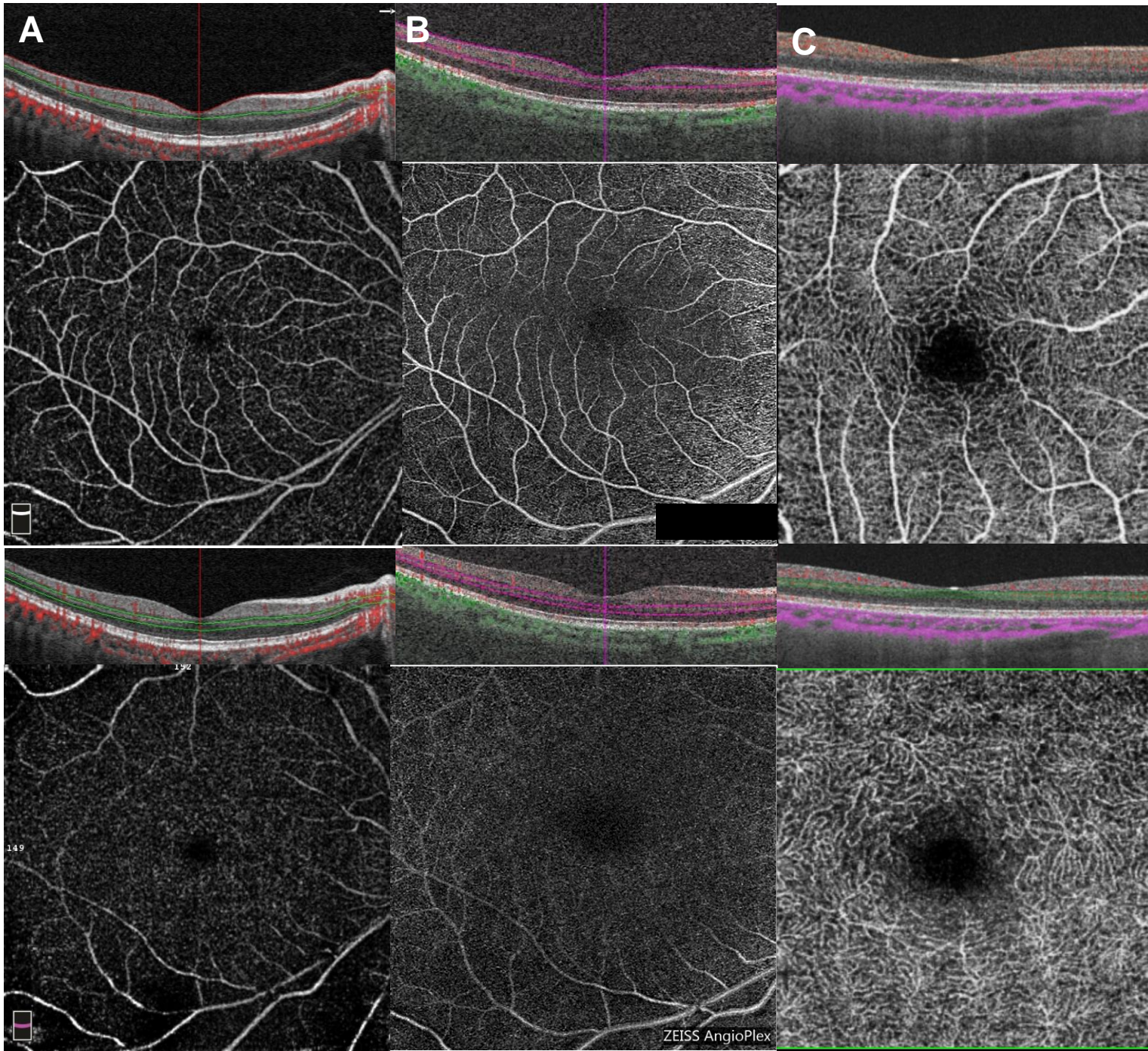
- 1298 46. Toto L, Borrelli E, Di Antonio L, Carpineto P, Mastropasqua R. Retinal Vascular  
1299 Plexuses' Changes in Dry Age-Related Macular Degeneration, Evaluated by Means  
1300 of Optical Coherence Tomography Angiography. *Retina*. 2016;36(8):1566-1572.
- 1301 47. Al-Sheikh M, Phasukkijwatana N, Dolz-Marco R, et al. Quantitative OCT  
1302 Angiography of the Retinal Microvasculature and the Choriocapillaris in Myopic  
1303 Eyes. *Investigative ophthalmology & visual science*. 2017;58(4):2063-2069.
- 1304 48. Querques L, Giuffre C, Corvi F, et al. Optical coherence tomography angiography of  
1305 myopic choroidal neovascularisation. *The British journal of ophthalmology*.  
1306 2017;101(5):609-615.
- 1307 49. Liu B, Bao L, Zhang J. Optical Coherence Tomography Angiography Of Pathological  
1308 Myopia Sourced and Idiopathic Choroidal Neovascularization With Follow-Up.  
1309 *Medicine*. 2016;95(14):e3264.
- 1310 50. Maruko I, Spaide RF, Koizumi H, et al. Choroidal Blood Flow Visualization in High  
1311 Myopia Using a Projection Artifact Method in Optical Coherence Tomography  
1312 Angiography. *Retina*. 2017;37(3):460-465.
- 1313 51. Dimitrova G, Chihara E, Takahashi H, Amano H, Okazaki K. Quantitative Retinal  
1314 Optical Coherence Tomography Angiography in Patients With Diabetes Without  
1315 Diabetic Retinopathy. *Investigative ophthalmology & visual science*.  
1316 2017;58(1):190-196.
- 1317 52. Soares M, Neves C, Marques IP, et al. Comparison of diabetic retinopathy  
1318 classification using fluorescein angiography and optical coherence tomography  
1319 angiography. *The British journal of ophthalmology*. 2017;101(1):62-68.
- 1320 53. Krawitz BD, Mo S, Geyman LS, et al. Acircularity index and axis ratio of the foveal  
1321 avascular zone in diabetic eyes and healthy controls measured by optical  
1322 coherence tomography angiography. *Vision research*. 2017.
- 1323 54. Ghasemi Falavarjani K, Iafe NA, Hubschman JP, Tsui I, Sadda SR, Sarraf D. Optical  
1324 Coherence Tomography Angiography Analysis of the Foveal Avascular Zone and  
1325 Macular Vessel Density After Anti-VEGF Therapy in Eyes With Diabetic Macular  
1326 Edema and Retinal Vein Occlusion. *Investigative ophthalmology & visual science*.  
1327 2017;58(1):30-34.
- 1328 55. Ishibazawa A, Nagaoka T, Takahashi A, et al. Optical Coherence Tomography  
1329 Angiography in Diabetic Retinopathy: A Prospective Pilot Study. *American journal  
1330 of ophthalmology*. 2015;160(1):35-44 e31.
- 1331 56. Salz DA, de Carlo TE, Adhi M, et al. Select Features of Diabetic Retinopathy on  
1332 Swept-Source Optical Coherence Tomographic Angiography Compared With  
1333 Fluorescein Angiography and Normal Eyes. *JAMA ophthalmology*.  
1334 2016;134(6):644-650.
- 1335 57. de Carlo TE, Chin AT, Bonini Filho MA, et al. Detection of Microvascular Changes  
1336 in Eyes of Patients with Diabetes but Not Clinical Diabetic Retinopathy Using  
1337 Optical Coherence Tomography Angiography. *Retina*. 2015;35(11):2364-2370.
- 1338 58. Takase N, Nozaki M, Kato A, Ozeki H, Yoshida M, Ogura Y. Enlargement of Foveal  
1339 Avascular Zone in Diabetic Eyes Evaluated by En Face Optical Coherence  
1340 Tomography Angiography. *Retina*. 2015;35(11):2377-2383.
- 1341 59. Samara WA, Shahlaee A, Adam MK, et al. Quantification of Diabetic Macular  
1342 Ischemia Using Optical Coherence Tomography Angiography and Its Relationship  
1343 with Visual Acuity. *Ophthalmology*. 2017;124(2):235-244.
- 1344 60. Ishibazawa A, Nagaoka T, Yokota H, et al. Characteristics of Retinal  
1345 Neovascularization in Proliferative Diabetic Retinopathy Imaged by Optical

- 1346 Coherence Tomography Angiography. *Investigative ophthalmology & visual*  
1347 *science*. 2016;57(14):6247-6255.
- 1348 61. Singh A, Agarwal A, Mahajan S, et al. Morphological differences between optic disc  
1349 collaterals and neovascularization on optical coherence tomography angiography.  
1350 *Graefe's archive for clinical and experimental ophthalmology = Albrecht von Graefes*  
1351 *Archiv fur klinische und experimentelle Ophthalmologie*. 2016.
- 1352 62. Hwang TS, Jia Y, Gao SS, et al. Optical Coherence Tomography Angiography  
1353 Features of Diabetic Retinopathy. *Retina*. 2015;35(11):2371-2376.
- 1354 63. Agemy SA, Sripsema NK, Shah CM, et al. Retinal Vascular Perfusion Density  
1355 Mapping Using Optical Coherence Tomography Angiography in Normals and  
1356 Diabetic Retinopathy Patients. *Retina*. 2015;35(11):2353-2363.
- 1357 64. Kim AY, Chu Z, Shahidzadeh A, Wang RK, Puliafito CA, Kashani AH. Quantifying  
1358 Microvascular Density and Morphology in Diabetic Retinopathy Using Spectral-  
1359 Domain Optical Coherence Tomography Angiography. *Investigative*  
1360 *ophthalmology & visual science*. 2016;57(9):OCT362-370.
- 1361 65. Zhang M, Hwang TS, Dongye C, Wilson DJ, Huang D, Jia Y. Automated  
1362 Quantification of Nonperfusion in Three Retinal Plexuses Using Projection-  
1363 Resolved Optical Coherence Tomography Angiography in Diabetic Retinopathy.  
1364 *Investigative ophthalmology & visual science*. 2016;57(13):5101-5106.
- 1365 66. Ting DS, Tan GS, Agrawal R, et al. Optical Coherence Tomographic Angiography in  
1366 Type 2 Diabetes and Diabetic Retinopathy. *JAMA ophthalmology*. 2017.
- 1367 67. Iafe NA, Phasukkijwatana N, Chen X, Sarraf D. Retinal Capillary Density and Foveal  
1368 Avascular Zone Area Are Age-Dependent: Quantitative Analysis Using Optical  
1369 Coherence Tomography Angiography. *Investigative ophthalmology & visual*  
1370 *science*. 2016;57(13):5780-5787.
- 1371 68. Bonini Filho MA, Adhi M, de Carlo TE, et al. Optical Coherence Tomography  
1372 Angiography in Retinal Artery Occlusion. *Retina*. 2015;35(11):2339-2346.
- 1373 69. Kashani AH, Lee SY, Moshfeghi A, Durbin MK, Puliafito CA. Optical Coherence  
1374 Tomography Angiography of Retinal Venous Occlusion. *Retina*.  
1375 2015;35(11):2323-2331.
- 1376 70. Kadomoto S, Muraoka Y, Ooto S, et al. EVALUATION OF MACULAR ISCHEMIA IN  
1377 EYES WITH BRANCH RETINAL VEIN OCCLUSION: An Optical Coherence  
1378 Tomography Angiography Study. *Retina*. 2017.
- 1379 71. Nobre Cardoso J, Keane PA, Sim DA, et al. Systematic Evaluation of Optical  
1380 Coherence Tomography Angiography in Retinal Vein Occlusion. *American journal*  
1381 *of ophthalmology*. 2016;163:93-107 e106.
- 1382 72. Coscas F, Glacet-Bernard A, Miere A, et al. Optical Coherence Tomography  
1383 Angiography in Retinal Vein Occlusion: Evaluation of Superficial and Deep  
1384 Capillary Plexa. *American journal of ophthalmology*. 2016;161:160-171 e161-162.
- 1385 73. Suzuki N, Hirano Y, Yoshida M, et al. Microvascular Abnormalities on Optical  
1386 Coherence Tomography Angiography in Macular Edema Associated With Branch  
1387 Retinal Vein Occlusion. *American journal of ophthalmology*. 2016;161:126-132  
1388 e121.
- 1389 74. de Castro-Abeger AH, de Carlo TE, Duker JS, Bauml CR. Optical Coherence  
1390 Tomography Angiography Compared to Fluorescein Angiography in Branch  
1391 Retinal Artery Occlusion. *Ophthalmic surgery, lasers & imaging retina*.  
1392 2015;46(10):1052-1054.

- 1393 75. Kang JW, Yoo R, Jo YH, Kim HC. Correlation of Microvascular Structures on Optical  
1394 Coherence Tomography Angiography with Visual Acuity in Retinal Vein Occlusion.  
1395 *Retina*. 2016.
- 1396 76. Casselholmde Salles M, Kvanta A, Amren U, Epstein D. Optical Coherence  
1397 Tomography Angiography in Central Retinal Vein Occlusion: Correlation Between  
1398 the Foveal Avascular Zone and Visual Acuity. *Investigative ophthalmology & visual  
1399 science*. 2016;57(9):OCT242-246.
- 1400 77. Sellam A, Glacet-Bernard A, Coscas F, Miere A, Coscas G, Souied EH. QUALITATIVE  
1401 AND QUANTITATIVE FOLLOW-UP USING OPTICAL COHERENCE TOMOGRAPHY  
1402 ANGIOGRAPHY OF RETINAL VEIN OCCLUSION TREATED WITH ANTI-VEGF:  
1403 Optical Coherence Tomography Angiography Follow-up of Retinal Vein Occlusion.  
1404 *Retina*. 2016.
- 1405 78. Matet A, Daruich A, Dirani A, Ambresin A, Behar-Cohen F. Macular Telangiectasia  
1406 Type 1: Capillary Density and Microvascular Abnormalities Assessed by Optical  
1407 Coherence Tomography Angiography. *Am J Ophthalmol*. 2016;167:18-30.
- 1408 79. Spaide RF, Klancnik JM, Jr., Cooney MJ, et al. Volume-Rendering Optical Coherence  
1409 Tomography Angiography of Macular Telangiectasia Type 2. *Ophthalmology*.  
1410 2015;122(11):2261-2269.
- 1411 80. Spaide RF, Suzuki M, Yannuzzi LA, Matet A, Behar-Cohen F. Volume-Rendered  
1412 Angiographic and Structural Optical Coherence Tomography Angiography of  
1413 Macular Telangiectasia Type 2. *Retina*. 2017;37(3):424-435.
- 1414 81. Chidambara L, Gadde SG, Yadav NK, et al. Characteristics and quantification of  
1415 vascular changes in macular telangiectasia type 2 on optical coherence  
1416 tomography angiography. *The British journal of ophthalmology*.  
1417 2016;100(11):1482-1488.
- 1418 82. Toto L, Di Antonio L, Mastropasqua R, et al. Multimodal Imaging of Macular  
1419 Telangiectasia Type 2: Focus on Vascular Changes Using Optical Coherence  
1420 Tomography Angiography. *Invest Ophthalmol Vis Sci*. 2016;57(9):OCT268-276.
- 1421 83. Denniston AK, Dick AD. Systemic therapies for inflammatory eye disease: past,  
1422 present and future. *BMC ophthalmology*. 2013;13:18.
- 1423 84. Kim AY, Rodger DC, Shahidzadeh A, et al. Quantifying Retinal Microvascular  
1424 Changes in Uveitis Using Spectral-Domain Optical Coherence Tomography  
1425 Angiography. *American journal of ophthalmology*. 2016;171:101-112.
- 1426 85. Levison AL, Baynes KM, Lowder CY, Kaiser PK, Srivastava SK. Choroidal  
1427 neovascularisation on optical coherence tomography angiography in punctate  
1428 inner choroidopathy and multifocal choroiditis. *The British journal of  
1429 ophthalmology*. 2016.
- 1430 86. Zahid S, Chen KC, Jung JJ, et al. Optical Coherence Tomography Angiography of  
1431 Chorioretinal Lesions Due to Idiopathic Multifocal Choroiditis. *Retina*. 2016.
- 1432 87. Cheng L, Chen X, Weng S, et al. Spectral-Domain Optical Coherence Tomography  
1433 Angiography Findings in Multifocal Choroiditis With Active Lesions. *American  
1434 journal of ophthalmology*. 2016;169:145-161.
- 1435 88. Chen KC, Marsiglia M, Dolz-Marco R, et al. Foveal Exudate and Choroidal  
1436 Neovascularization in Atypical Cases of Multiple Evanescent White Dot Syndrome.  
1437 *Retina*. 2017.
- 1438 89. de Carlo TE, Bonini Filho MA, Adhi M, Duker JS. Retinal and Choroidal Vasculature  
1439 in Birdshot Chorioretinopathy Analyzed Using Spectral Domain Optical Coherence  
1440 Tomography Angiography. *Retina*. 2015;35(11):2392-2399.

- 1441 90. Roberts PK, Nesper PL, Goldstein DA, Fawzi AA. Retinal Capillary Density in  
1442 Patients with Birdshot Chorioretinopathy. *Retina*. 2017.
- 1443 91. Khairallah M, Abroug N, Khochtali S, et al. Optical Coherence Tomography  
1444 Angiography in Patients with Behcet Uveitis. *Retina*. 2016.
- 1445 92. Aggarwal K, Agarwal A, Deokar A, et al. Distinguishing features of acute Vogt-  
1446 Koyanagi-Harada disease and acute central serous chorioretinopathy on optical  
1447 coherence tomography angiography and en face optical coherence tomography  
1448 imaging. *Journal of ophthalmic inflammation and infection*. 2017;7(1):3.
- 1449 93. Heiferman MJ, Rahmani S, Jampol LM, et al. Acute Posterior Multifocal Placoid  
1450 Pigment Epitheliopathy on Optical Coherence Tomography Angiography. *Retina*.  
1451 2017.
- 1452 94. Pichi F, Srivastava SK, Levinson A, Baynes KM, Traut C, Lowder CY. A Focal  
1453 Chorioretinal Bartonella Lesion Analyzed by Optical Coherence Tomography  
1454 Angiography. *Ophthalmic Surg Lasers Imaging Retina*. 2016;47(6):585-588.
- 1455 95. Jia Y, Wei E, Wang X, et al. Optical coherence tomography angiography of optic  
1456 disc perfusion in glaucoma. *Ophthalmology*. 2014;121(7):1322-1332.
- 1457 96. Liu L, Jia Y, Takusagawa HL, et al. Optical Coherence Tomography Angiography of  
1458 the Peripapillary Retina in Glaucoma. *JAMA ophthalmology*. 2015;133(9):1045-  
1459 1052.
- 1460 97. Yarmohammadi A, Zangwill LM, Diniz-Filho A, et al. Relationship between Optical  
1461 Coherence Tomography Angiography Vessel Density and Severity of Visual Field  
1462 Loss in Glaucoma. *Ophthalmology*. 2016;123(12):2498-2508.
- 1463 98. Akil H, Huang AS, Francis BA, Sadda SR, Chopra V. Retinal vessel density from  
1464 optical coherence tomography angiography to differentiate early glaucoma, pre-  
1465 perimetric glaucoma and normal eyes. *PLoS One*. 2017;12(2):e0170476.
- 1466 99. Ang M, Sng C, Milea D. Optical coherence tomography angiography in dural  
1467 carotid-cavernous sinus fistula. *BMC Ophthalmol*. 2016;16:93.
- 1468 100. Sharma S, Ang M, Najjar RP, et al. Optical coherence tomography angiography in  
1469 acute non-arteritic anterior ischaemic optic neuropathy. *The British journal of*  
1470 *ophthalmology*. 2017.
- 1471 101. Ghasemi Falavarjani K, Tian JJ, Akil H, Garcia GA, Sadda SR, Sadun AA. Swept-  
1472 Source Optical Coherence Tomography Angiography of the Optic Disk in Optic  
1473 Neuropathy. *Retina*. 2016;36 Suppl 1:S168-S177.
- 1474 102. Wang X, Jia Y, Spain R, et al. Optical coherence tomography angiography of optic  
1475 nerve head and parafovea in multiple sclerosis. *The British journal of*  
1476 *ophthalmology*. 2014;98(10):1368-1373.
- 1477 103. Higashiyama T, Nishida Y, Ohji M. Optical coherence tomography angiography in  
1478 eyes with good visual acuity recovery after treatment for optic neuritis. *PLoS one*.  
1479 2017;12(2):e0172168.
- 1480 104. Ang M, Cai Y, Shahipasand S, et al. En face optical coherence tomography  
1481 angiography for corneal neovascularisation. *Br J Ophthalmol*. 2015.
- 1482 105. Ang M, Sim DA, Keane PA, et al. Optical Coherence Tomography Angiography for  
1483 Anterior Segment Vasculature Imaging. *Ophthalmology*. 2015;122(9):1740-1747.
- 1484 106. Ang M, Cai Y, Tan AC. Swept Source Optical Coherence Tomography Angiography  
1485 for Contact Lens-Related Corneal Vascularization. *J Ophthalmol*.  
1486 2016;2016:9685297.
- 1487 107. Ang M, Cai Y, MacPhee B, et al. Optical coherence tomography angiography and  
1488 indocyanine green angiography for corneal vascularisation. *Br J Ophthalmol*.  
1489 2016.

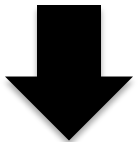
- 1490 108. Ang M, Cai Y, Shahipasand S, et al. En face optical coherence tomography  
1491 angiography for corneal neovascularisation. *Br J Ophthalmol.* 2016;100(5):616-  
1492 621.
- 1493 109. Ploner SB, Moulton EM, Choi W, et al. TOWARD QUANTITATIVE OPTICAL  
1494 COHERENCE TOMOGRAPHY ANGIOGRAPHY: Visualizing Blood Flow Speeds in  
1495 Ocular Pathology Using Variable Interscan Time Analysis. *Retina.* 2016;36 Suppl  
1496 1:S118-S126.  
1497



**ASSESS THE SCAN  
QUALITY**



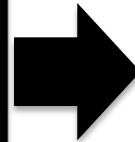
**IDENTIFY AREA  
AND LAYER OF  
INTEREST**



**EXAMINE CROSS-  
SECTIONAL  
OCTA FOR  
ABNORMAL  
FLOW**



**CHOOSE  
SEGMENTATION  
PATTERN THAT BEST  
CAPTURES  
ABNORMAL FLOW**



**MANUAL  
MANIPULATION OF  
SEGMENTATION TO  
OPTIMISE ENFACE  
OCTA IMAGE**

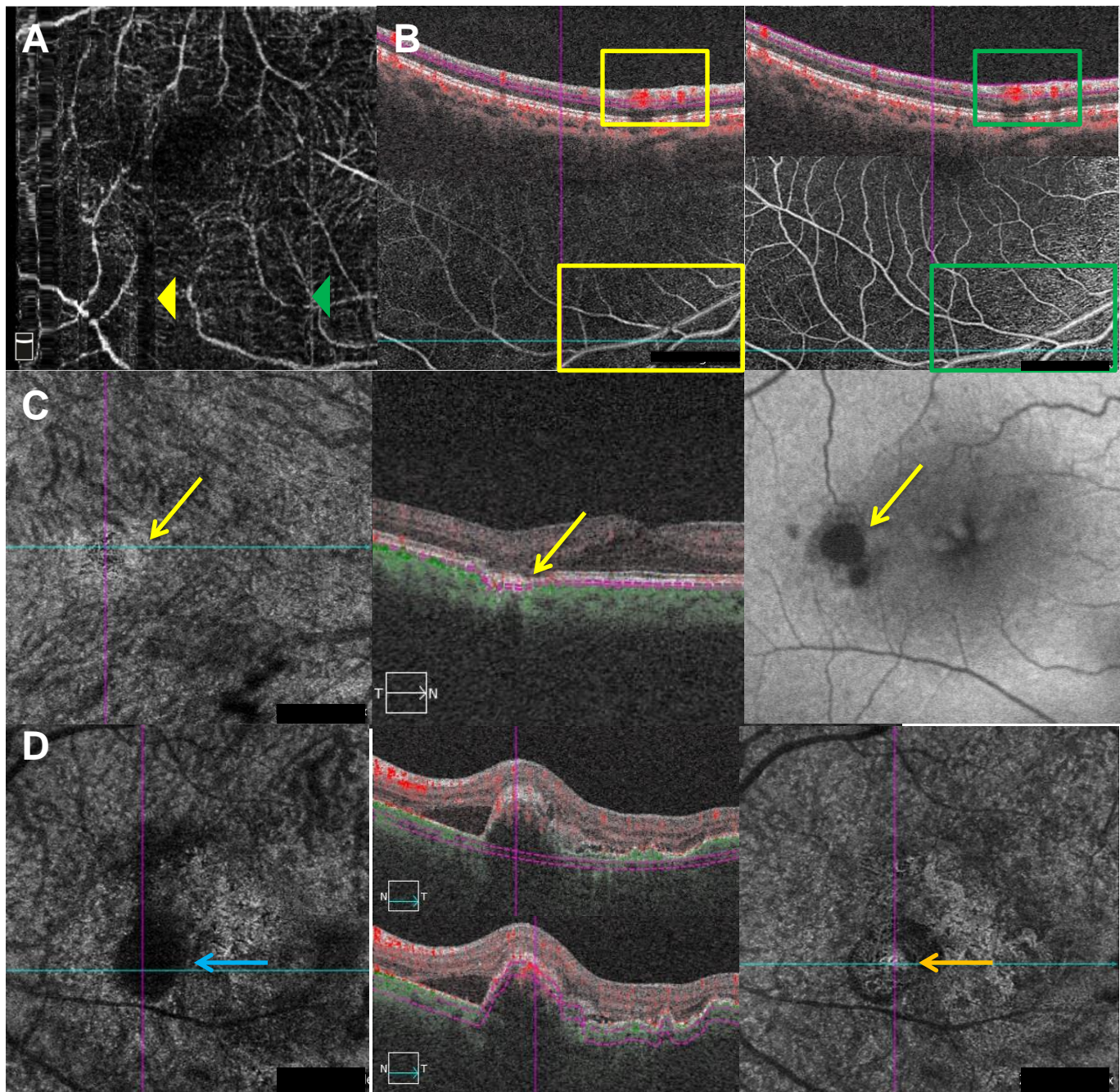


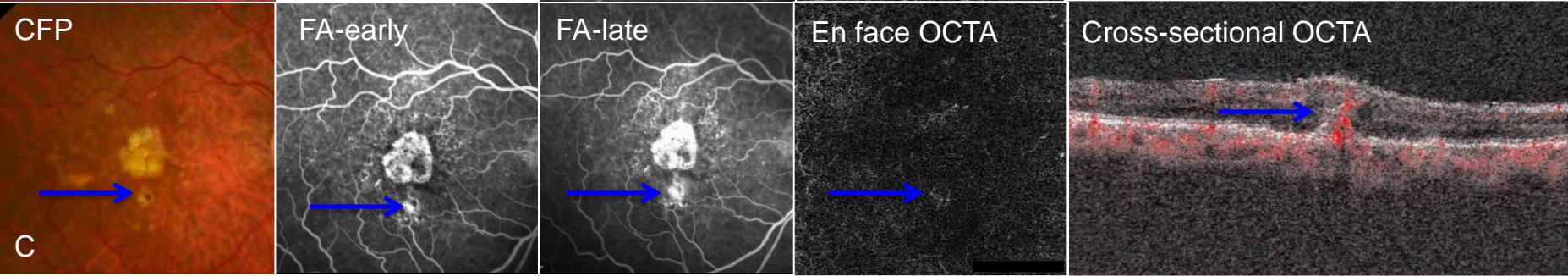
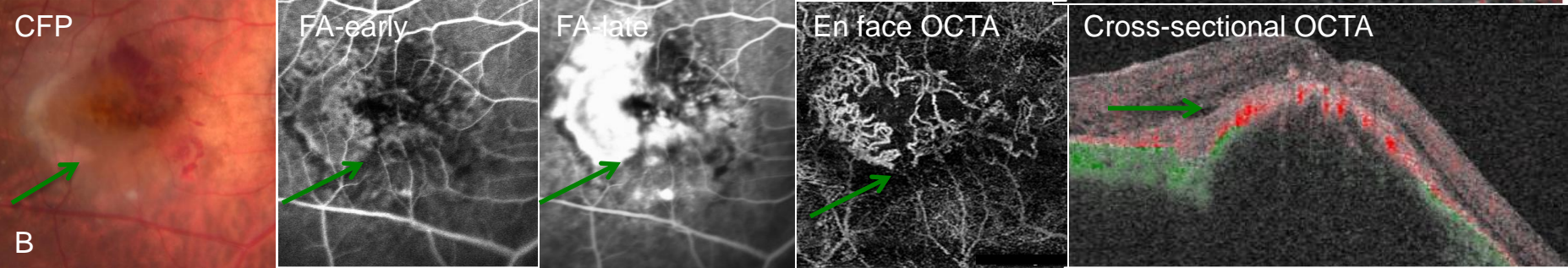
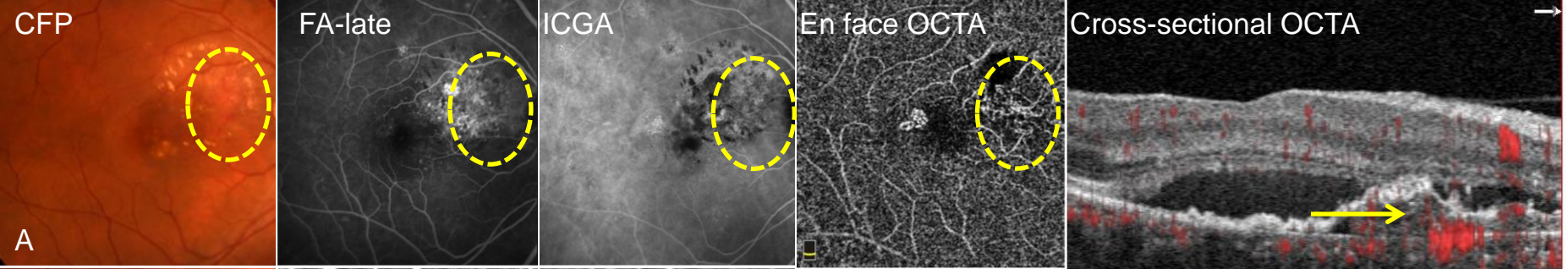
**CORRELATE TO  
OTHER IMAGING  
MODALITIES**

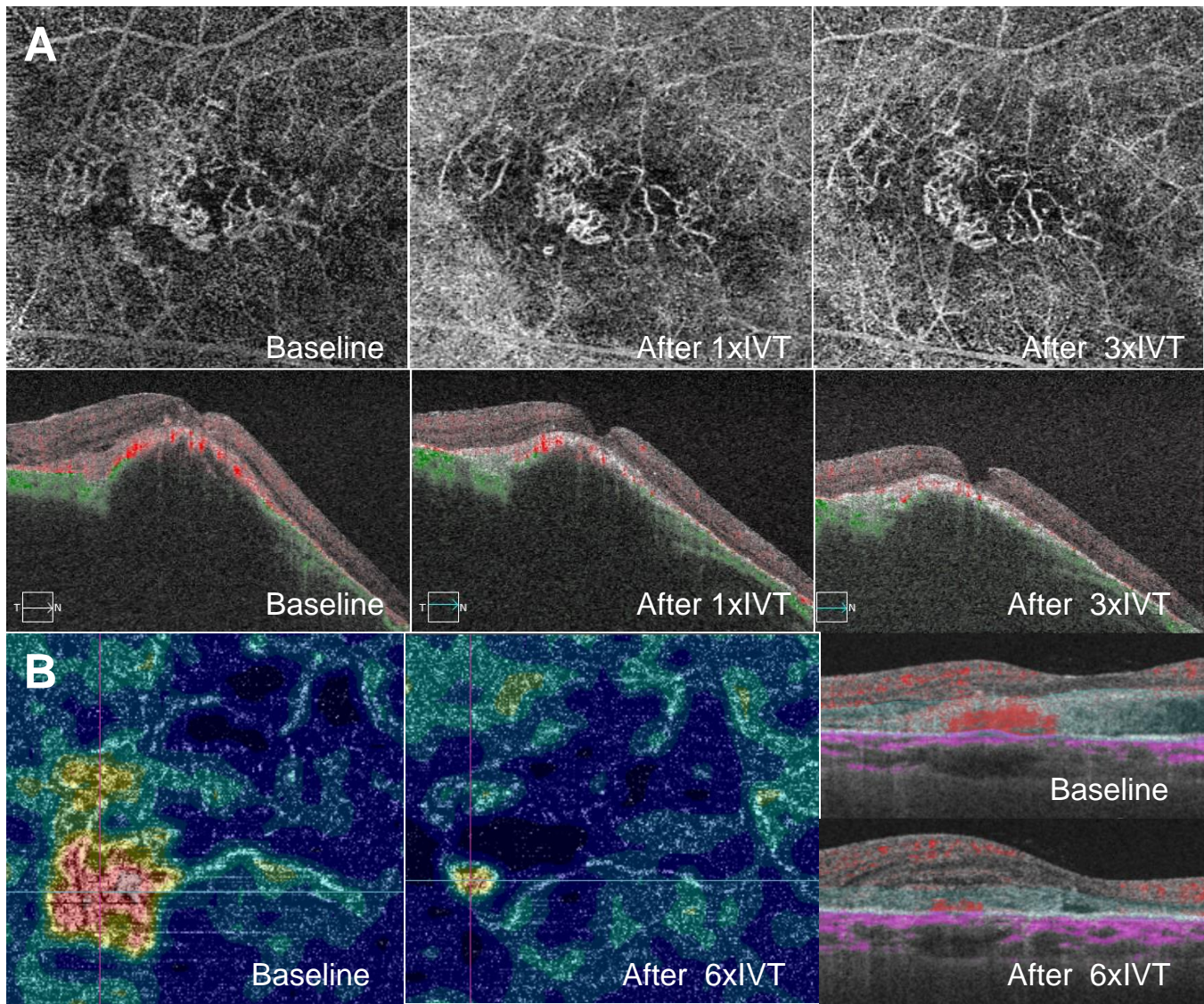


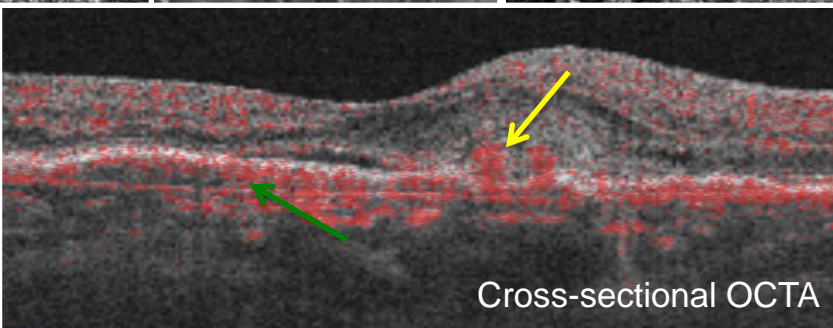
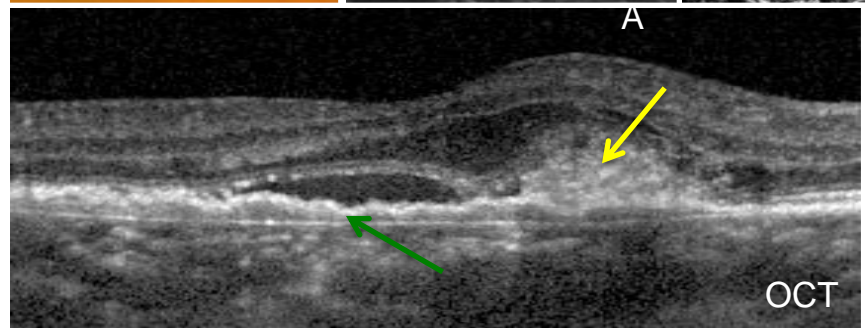
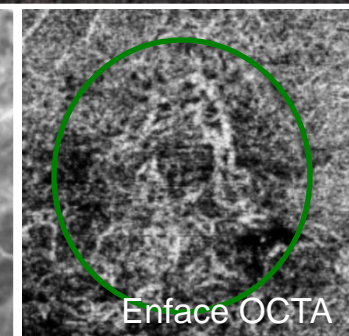
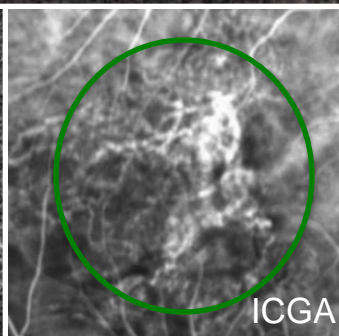
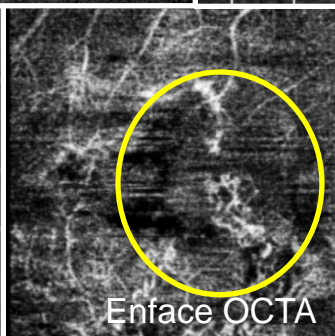
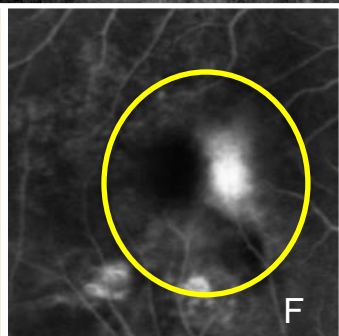
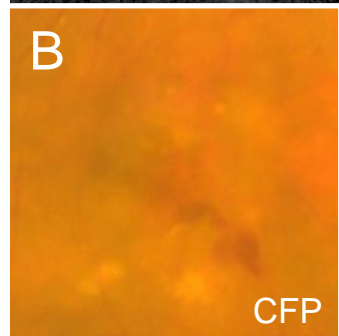
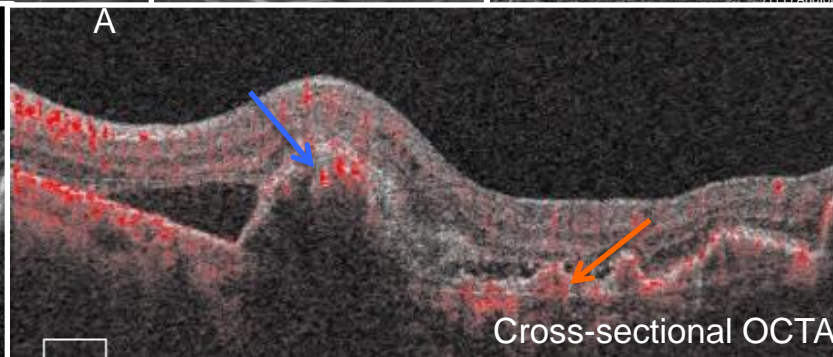
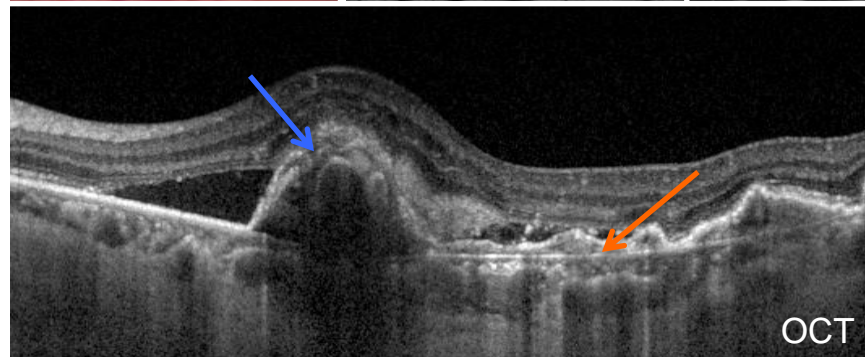
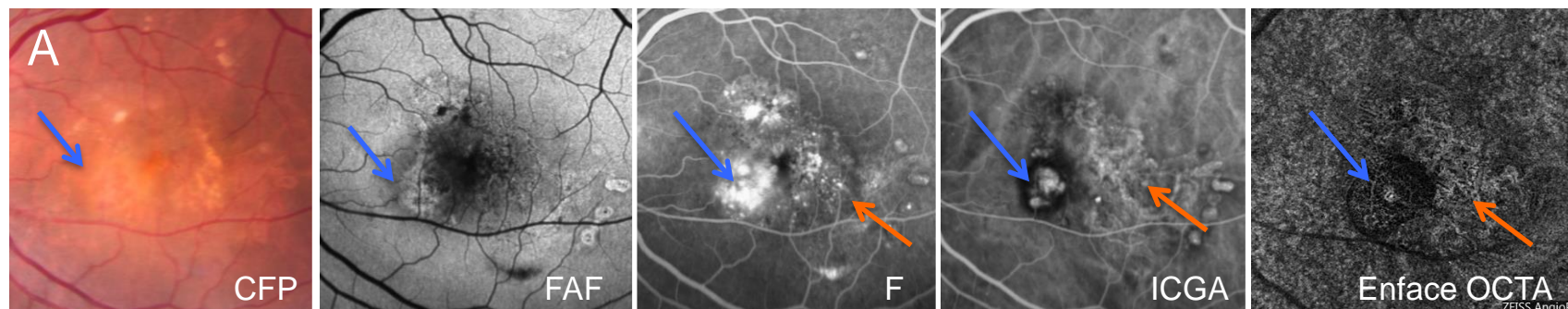
**BE MINDFUL OF  
ARTEFACTS**

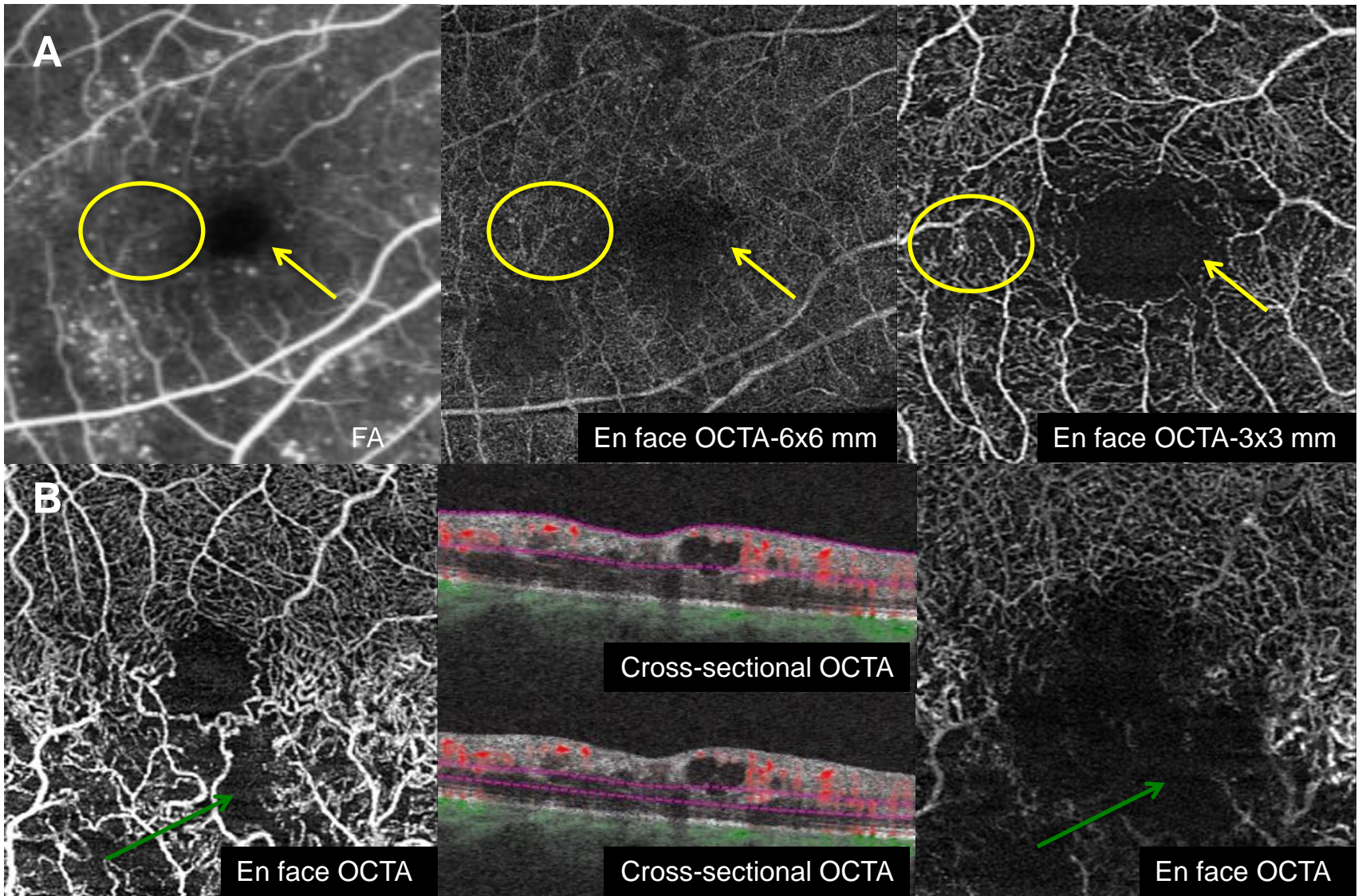
**AN APPROACH TO OCTA  
INTEPRETATION**

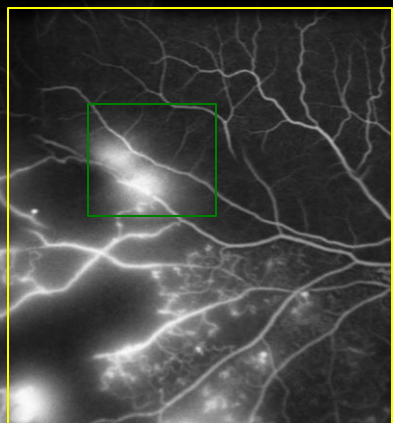




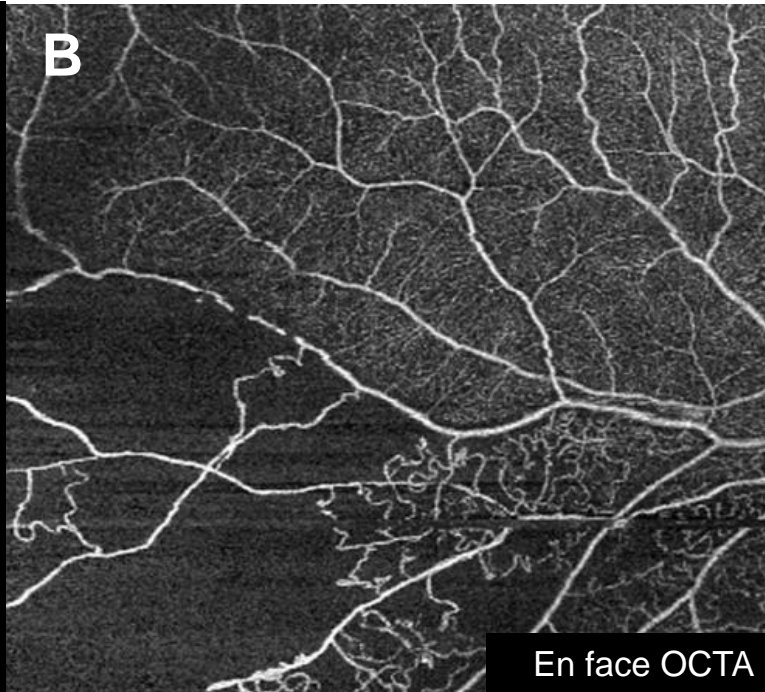






**A**

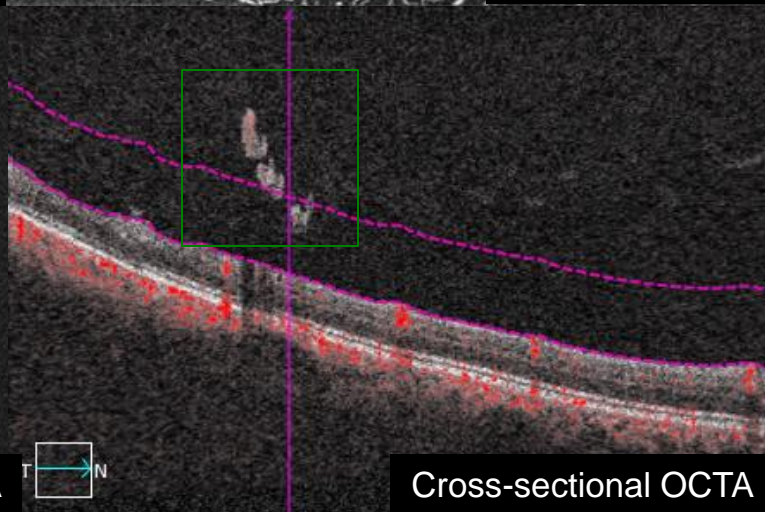
FA

**B**

En face OCTA

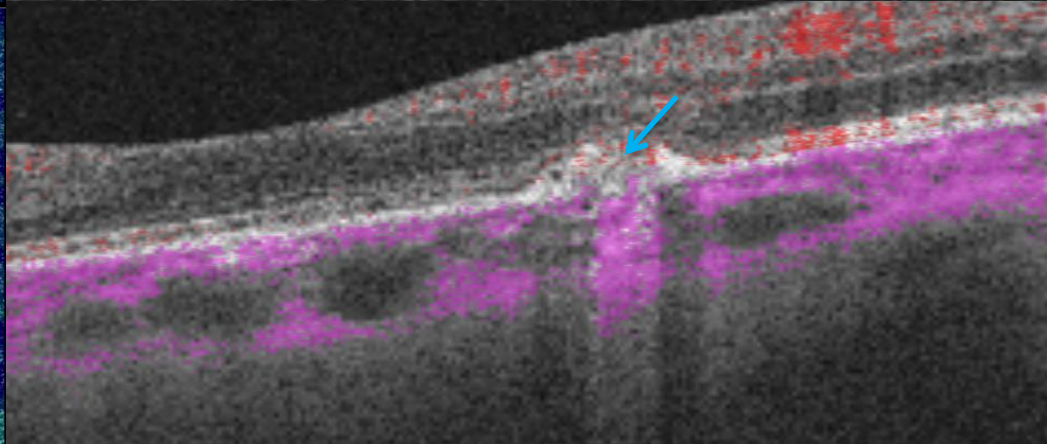
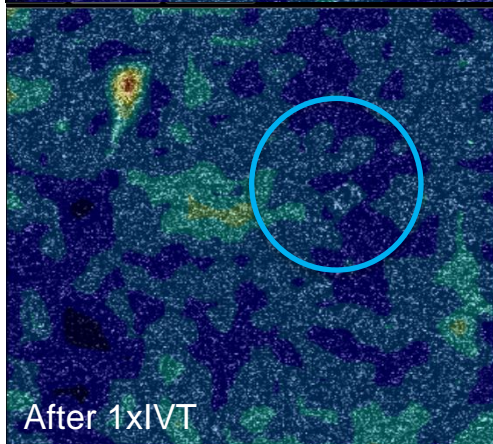
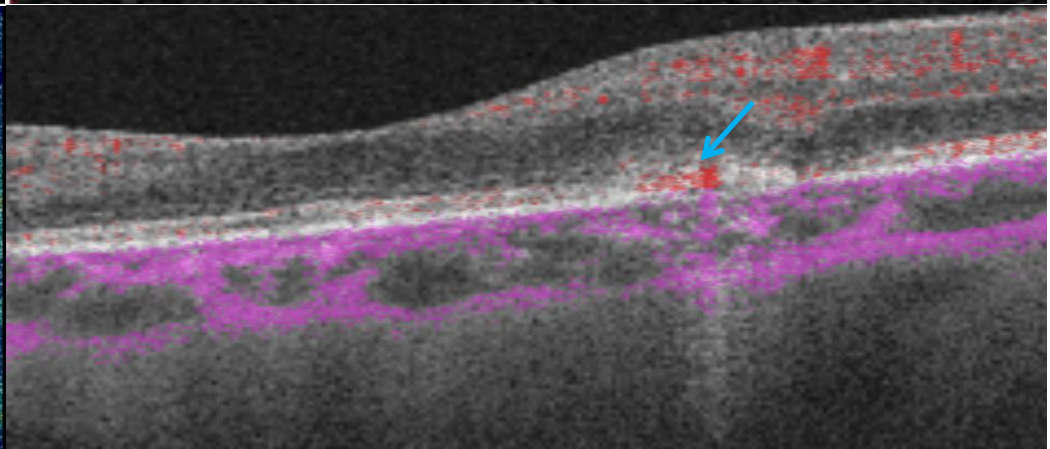
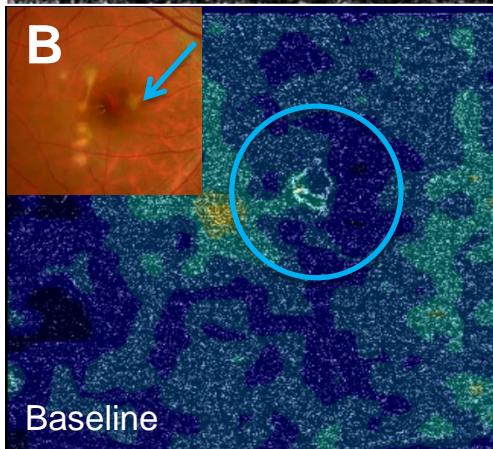
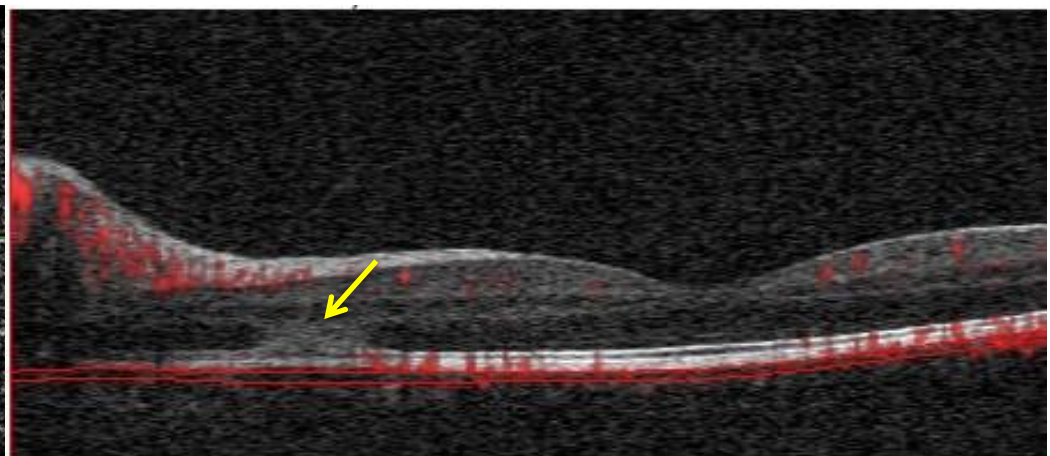
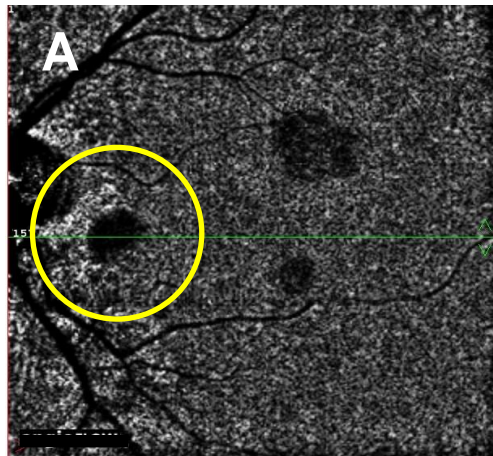
**C**

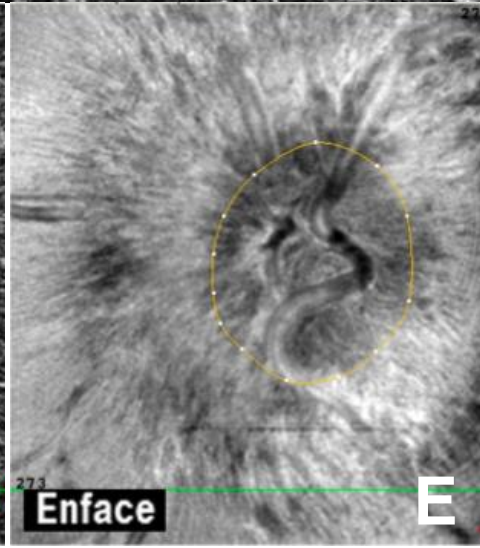
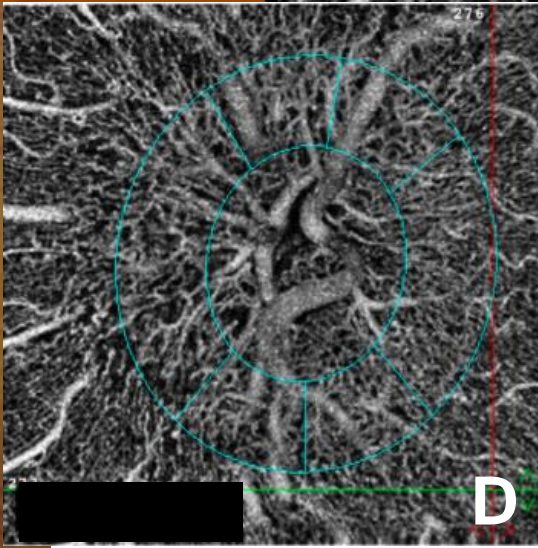
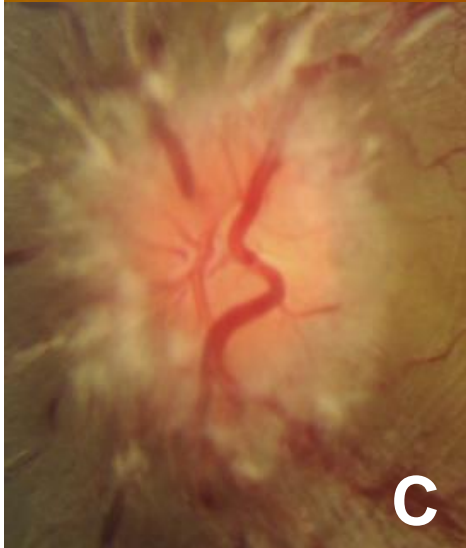
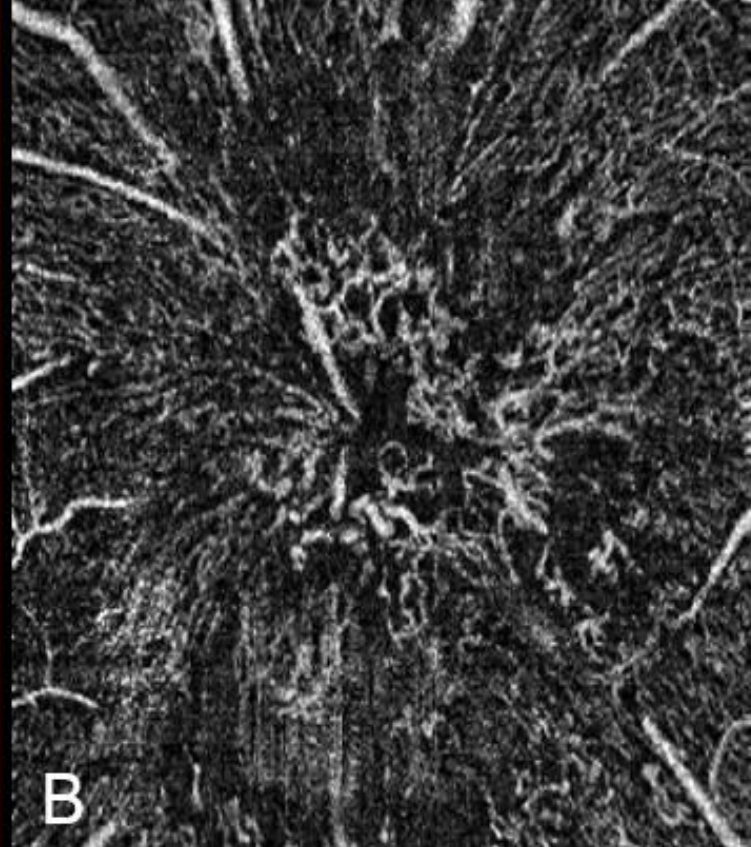
En face OCTA



Cross-sectional OCTA







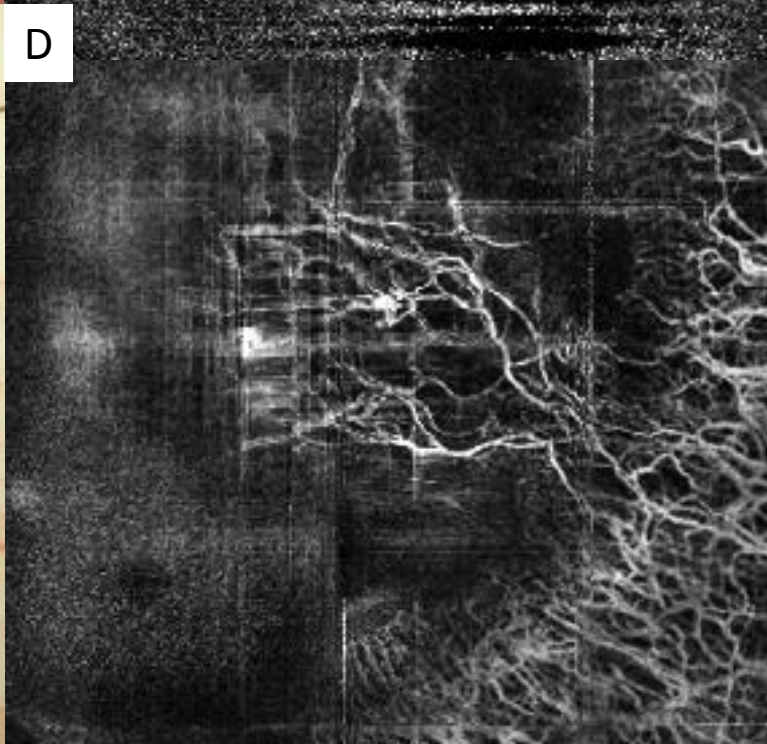
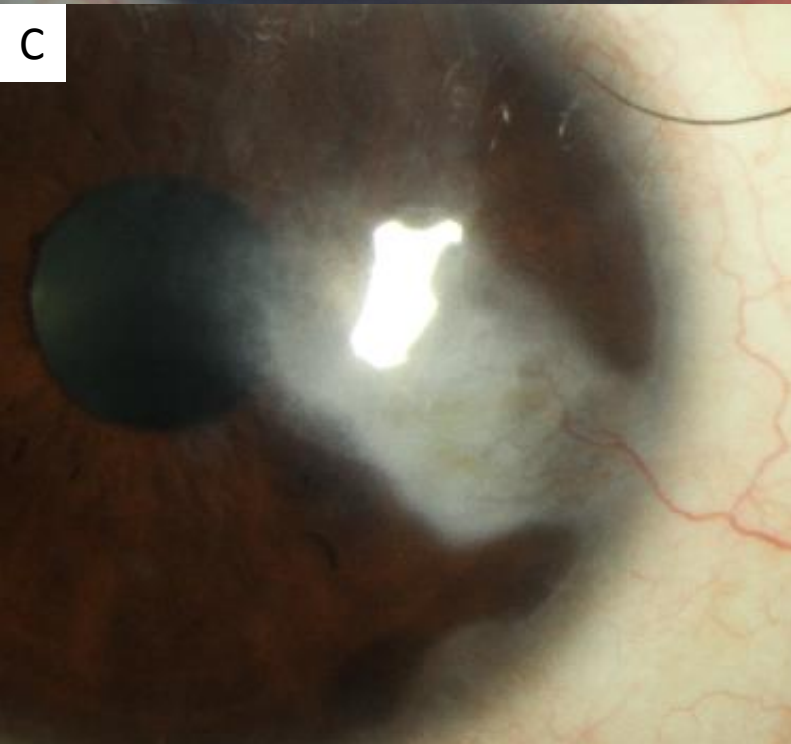
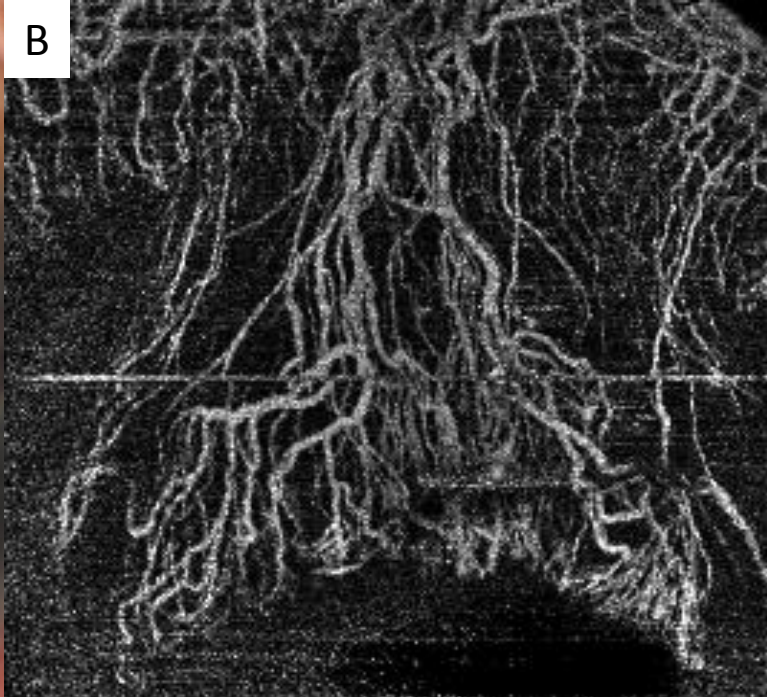
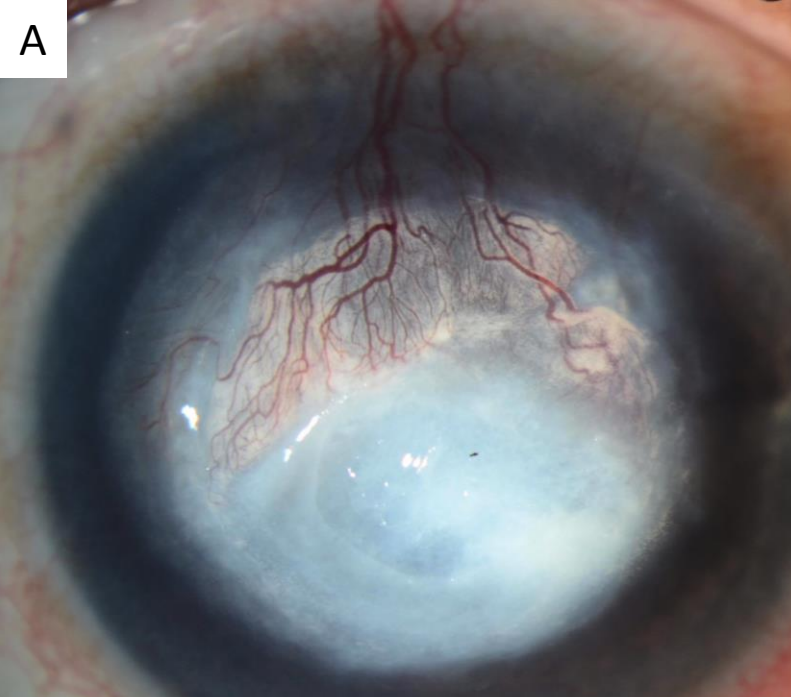


Table 1: Comparison of optical coherence tomography angiography (OCTA) versus conventional angiography such as fundus fluorescein angiography (FFA) and indocyanine green angiography (ICGA).

OCTA	FFA	ICGA
New technology not validated	Well validated technology	Well validated technology
	Correlation to multi-modal imaging and histology	Correlation to multi-modal imaging and histology
Non-invasive, no need for dye	Invasive, need for dye risk of anaphylaxis	Invasive, need for dye risk of anaphylaxis
Rapid acquisition time	Time-consuming to perform	Time-consuming to perform
Interpretation may require more time	Image viewing may be faster	Image viewing may be faster
Provides depth information of both retinal and choroidal vasculature	No information about individual layers	No information about individual layers
Able to segment various layers	Retina imaged in entirety	Choroid imaged in entirety
Able to image through blood	Blockage from blood	Able to penetrate blood
Artifacts may hamper interpretation	Less artifact	Less artifact
Detection of flow but not leakage	Detection of leakage and activity	Detection of leakage and activity
High resolution down to capillaries in the retina	Lower resolution, able to image large retinal vessels but not capillaries	Able to image large choroidal vessels but not choriocapillaries
Small field of view	Wide field option available	Wide-field option available
No stereoscopic function	Stereoscopic option	Stereoscopic option
No dynamic video function	Video function available	Video function available

Table 2: Comparison of four current commercially available optical coherence tomography angiography (OCTA) platforms and their various specifications (Information up to date as of January 2017).

<b>Specifications</b>	<b>AngioVue</b>	<b>Angioplex</b>	<b>Spectralis OCTA</b>	<b>SS OCT Angio</b>	<b>Angioscan</b>
<b>OCT platform</b>	AngioVue RTVue XR Avanti	CIRRUS HD-OCT Model 5000	Spectralis OCT-2	DRI-OCT Triton swept source OCT	RS-3000 Advance
<b>Imaging company</b>	Optovue	Carl Zeiss Meditec, Inc	Heidelberg Engineering	Topcon Corporation	Nidek
<b>Place of origin</b>	Fremont, California, USA	Dublin, California, USA	Heidelberg, Germany	Tokyo, Japan	Gamagori, Aichi, Japan
<b>Scanning speed</b>	70,000 scans/sec	68,000 scans/sec	85,000 scans/sec	100,000 scans/sec	53,000 scans/sec
<b>Scanning volume</b>	304x304 A scans	245x245, 350x350 A scans	512x512 A scans	320x320, 512x512 A scans	256x256 A scans
<b>Algorithm</b>	Split-spectrum amplitude-decorrelation angiography (SSADA)	Optical coherence microangiography-complex (OMAG)	Probabilistic Model that predicts whether a voxel contained flow or not.	OCTA- Ratio Analysis (full spectrum amplitude)	Complex difference (full spectrum amplitude)
<b>Type of algorithm</b>	Amplitude	Amplitude+phase	Probabilistic model	Amplitude	Amplitude +phase
<b>Scan area (macula)</b>	3x3, 6x6, 8x8 mm	3x3, 6x6, 8x8 mm	3x3 mm with (5.7 x 5.7) $\mu\text{m}/\text{px}$	3x3, 4.5x4.5, 6x6, 9x9 mm	3x3-9x9mm (12x9 montage)
<b>Optical Resolution</b>					
• <b>Axial</b>	3 $\mu\text{m}$	5 $\mu\text{m}$	7 $\mu\text{m}$	8 $\mu\text{m}$	7 $\mu\text{m}$
• <b>Lateral</b>	15 $\mu\text{m}$	15 $\mu\text{m}$	14 $\mu\text{m}$	20 $\mu\text{m}$	20 $\mu\text{m}$
• <b>Light source</b>	840nm	840nm	880nm	1050nm	880nm
• <b>Axial imaging depth</b>	2-3mm	2mm	1.9mm	2.6mm	2.1mm

<b>Automated segmentation options</b>	Superficial retinal capillary plexus Deep retinal capillary plexus Outer Retina Choriocapillaries	Retina depth encoded Vitreo-retinal interface Superficial retina Deep retina Avascular layer Choriocapillaris Choroid	4 presets matching vasculature in retinal nerve fibre layer, ganglion cell layer and bracketing the inner nuclear layer  3 presets to cover the retina (Superficial, Deep Vascular Plexus and Avascular Layer)	Superficial vascular plexus Deep vascular plexus Outer retina Choriocapillaris	Superficial retinal layer Deep retinal layer Avascular Choriocapillaris
<b>Color coding of segmentations</b>	Yes	Yes	Yes	Yes	Yes
<b>Cross sectional OCTA image</b>	Yes	Yes	Yes	Yes	No
<b>Eye tracker</b>	Software update for older models Available with newer models	Yes (Fast Trac)	Yes (TruTrack)	Yes (Smart Track)	Yes
<b>Motion correction</b>	Yes (Motion Tracker)	N/A	Covered by TruTrack	Yes	Yes (real-time SLO eye tracking)
<b>Projection artifact removal</b>	Yes	Yes	Under development	Yes	Yes
<b>Optic nerve OCTA</b>	Yes	Yes	Yes	Yes	Yes
<b>Anterior segment OCTA function</b>	Prototype	Under development	No	No	Yes
<b>Quantitative analysis</b>	Yes	Yes	Under development	Yes (prototype)	Yes
<b>Comparative follow-up function</b>	Yes	Yes	Yes	Yes	No

Table 3: Multimodal characteristics of atrophic age-related macular degeneration (AMD) and subtypes of neovascular AMD

Imaging modality	Atrophic AMD	Neovascular AMD			
		Type 1 NV	BVN+PCV	Type 2 NV	Type 3 NV
CFP	Area of depigmentation	Blood, exudation, PED	Blood, exudation PED, orange nodule	Blood, exudation, greyish membrane	Pigmentary changes, exudation, blood
FAF	Hypoautofluorescence area Hyperfluorescent border	Variable	Variable	Variable	Not seen
FA	Window defect	Stippled hyperfluorescence with late diffuse leakage	Stippled hyperfluorescence with late diffuse leakage in the BVN	Early lacy pattern with late leakage	Focal areas of early leakage with right angled vessels
ICGA	Hypercyanescence in area of atrophy due to a window defect	Hypercyanescent plaque	Focal areas of hypercyanescence (polyps) with adjacent plaque	Not well defined	Retina choroidal anastomosis
OCT	Loss of the hyperreflective RPE band and outer retinal layers	Multi-layered PED Subretinal fluid and subretinal hyperreflective material	Focal elevated peaked PED (polyp) associated serous PED or shallow irregular PED (BVN) Subretinal fluid	Subretinal hyper-reflective material (SHRM) Subretinal fluid	Linear hyperreflective structure in the outer retina Intraretinal fluid
Cross sectional OCTA	High flow signal in the choroid beneath the area of RPE atrophy	Intrinsic flow signal within the PED	Focal areas of flow within the PED with high flow signal within BVN	Intrinsic flow seen within SHRM	Intrinsic linear flow within the hyperreflective structure High flow tuft
En face OCTA	Unmasking artefact with the atrophic area showing an increased flow signal	A tangle of vessels	Variable flow within polyps BVN seen as a tangle of vessels	A tangle of vessels	

AMD=age-related macula degeneration, NV=neovascularization, BVN=branching vascular network, CFP=color fundus photo,  
PED=pigment epithelial detachment, FAF=fundus autofluorescence, FA=fluorescein angiography, ICGA=indocyanine green angiography,  
OCT=optical coherence tomography, OCTA= optical coherence tomography tomography,